

TensorCommitments: A Lightweight Verifiable Inference for Language Models

Oguzhan Baser¹ Elahe Sadeghi¹ Eric Wang² David Ribeiro Alves² Sam Kazemian² Hong Kang³
Sandeep P. Chinchali¹ Sriram Vishwanath⁴

Abstract

Most large language models (LLMs) run on external clouds: users send a prompt, pay for inference, and must trust that the remote GPU executes the LLM without any adversarial tampering. We critically ask how to achieve verifiable LLM inference, where a prover (the service) must convince a verifier (the client) that an inference was run correctly without rerunning the LLM. Existing cryptographic works are too slow at the LLM scale, while non-cryptographic ones require a strong verifier GPU. We propose TensorCommitments (TCs), a tensor-native proof-of-inference scheme. TC binds the LLM inference to a commitment, an irreversible tag that breaks under tampering, organized in our multivariate Terkle Trees. For LLaMA2, TC adds only 0.97% prover and 0.12% verifier time over inference while improving robustness to tailored LLM attacks by up to 48% over the best prior work requiring a verifier GPU.

1. Introduction

As large language models (LLMs) move from *chatbots to decision-makers*, we increasingly have to **trust** remote inference runs that we cannot see or replay. Today, LLMs help draft code and execute tools in software pipelines, coordinate multi-agent workflows, and support decisions in finance, healthcare, and law (Wang et al., 2024). In many of these settings, an LLM runs on external infrastructure, produces a stream of tokens, and *downstream systems act on those tokens as if they were ground truth*. If the underlying computation is *silently corrupted* - by hardware faults, misconfiguration, or even a compromised service - agents may trade on the wrong market signal, a medical assistant may summarize the wrong patient record, or an autonomous system may reason over tampered state (Wang et al., 2024).

¹Electrical and Computer Engineering, The University of Texas at Austin ²Theseus AI Labs ³Electrical and Computer Engineering, McGill University ⁴Electrical and Computer Engineering, Georgia Institute of Technology. Correspondence to: Oguzhan Baser <oguzhanbaser@utexas.edu>.

Copyright 2026 by the author(s).

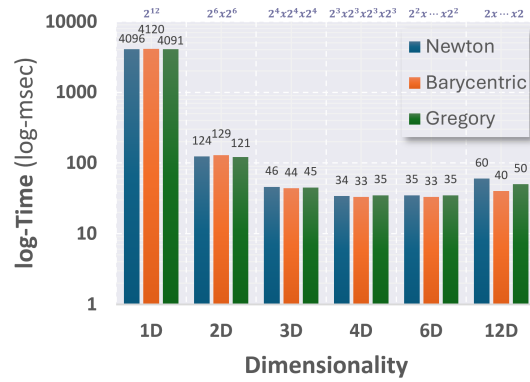


Figure 1. The key observation behind our TensorCommitments: multivariate interpolation is faster. We plot log-runtime to interpolate a polynomial over a fixed grid of $N = 2^{12}$ samples, reshaped from 1D (2^{12} points) to m D grids ($2^{\frac{12}{m}} \times \dots \times 2^{\frac{12}{m}}$) using Newton, Barycentric, and Gregory interpolation. Across all, moving from univariate ($m = 1$) to bivariate ($m = 2$) cuts runtime from 4.1s to 0.125s (over $\mathbf{30}\times$ speedup), with further reductions as dimension increases. Its time bound $\mathcal{O}((\frac{m+1}{m})^2)$ derived in App. H, decreases sharply as the tensor dimension m grows.

Current deployments provide almost **no traceability** of the intermediate activations or hidden states of these billion-parameter models; only the final text is visible, and re-running the full model just to check every answer is prohibitively expensive. As LLM usage scales to persistent, tool-using, and multi-agent systems, the gap between the *impact* of a single faulty inference and our ability to cheaply verify it is widening (Li et al., 2024). This motivates the **central question** of this work: *can we design a practical mechanism that allows lightweight clients to check whether a complex LLM inference was executed correctly, without rerunning the model or exposing its internal states?*

Existing works on verifiable LLMs *only partially* address this and runs into *sharp trade-offs* between scalability, privacy, and verifier cost. Cryptographic systems based on *zero-knowledge proofs* (Sun et al., 2024; Chen et al., 2024; Kang et al., 2023; Lee et al., 2022; Liu et al., 2021; Weng et al., 2021) can certify end-to-end correctness of an inference while hiding model parameters, but by compiling every tensor operation into a large constraint system. For LLM-

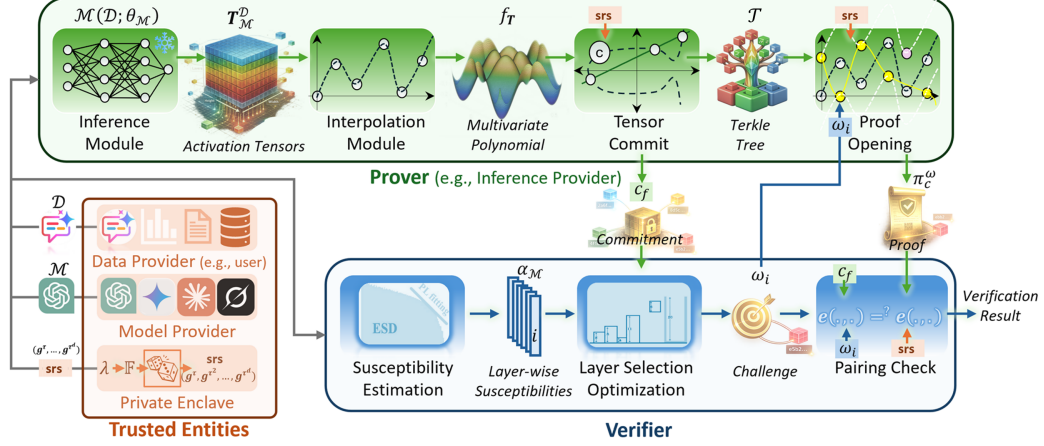


Figure 2. How does our verifiable inference pipeline work? *Trusted setup:* A secure enclave publishes structured reference string $srs = (g^{\tau}, g^{\tau^2}, \dots)$ with the model and data. *Prover:* Runs model $M(D; \theta_M)$ to produce activation tensors T_M^D ; interpolates into multivariate polynomial f_T ; commits to obtain C_f and builds Terkle tree T ; upon verifier challenge ω_i , provides opening proofs $\pi_C^{\omega_i}$. *Verifier:* Uses spectral heavy-tail scores α_M to rank layers, solves the interval selector, Problem 4.5, to choose challenge $\{\omega_i\}$, and checks pairing $e(\cdot, \cdot)$, accepting only if all checks pass. The prover does all heavy work. The verifier checks pairings and *does not* re-run full inference.

scale models, this leads to minutes of prover run-time per query and huge extra compute compared to plain inference, which is hard to amortize in interactive or multi-agent workloads. In parallel, *learning-based works* (Sun et al., 2025; Qi et al., 2025), train auxiliary models to detect perturbed outputs, or “critique” reasoning traces, but their guarantees are statistical rather than cryptographic. Also, they need retraining or finetuning whenever the base model or domain shifts. A recent ICML work, TOPLOC (Ong et al., 2025), takes a more practical route and fits last activations to a polynomial to detect model, prompt, or precision changes with low storage overhead, but the verifier still needs to recompute the forward pass with access to model weights and substantial GPU memory. It exposes internal states and thus violates user privacy. Further, these schemes flatten the compute into vectors, checking correctness per token instead of maintaining the tensor layout (e.g., spatiotemporal grids) (Ghodsi et al., 2017). This vector-centric view inflates the proof size with each new dimension and offers no direct way to reason about localized changes, motivating a tensor-native scheme that scales to LLMs with light-compute verifiers.

Our **key technical insight** is that commitment schemes are conceptually well matched to verifiable inference: if each hidden state and parameter block is bound to a succinct commitment, a remote run can be verified with a few proofs rather than replaying the full model. However, existing constructions are fundamentally *vector*-centric: they encode long flat vectors with *univariate polynomials* (Kate et al., 2010). For billion-parameter LLMs, the polynomial degree and the committed vectors grow with every layer and token, so interpolation rapidly dominates the cost, even without multi-agent interactions. Our **key observation** is that this

bottleneck stems from *the univariate view*, not from commitments themselves. By viewing parameters as tensors and committing to *multivariate* polynomials to respect their natural axes (e.g., layers and heads), we preserve tensor structure and exploit fast multivariate evaluation to keep commitments and proofs efficient. Fig. 1 shows this core scaling behavior: *for fixed data, multivariate interpolation becomes substantially more efficient than univariate one as dimensionality increases*. This makes tensor-native commitments a **natural fit** for LLM workloads. Fig. 2 gives the overview: a model host attaches *TensorCommitments*, organizes them into *an authenticated tree*, and streams compact proofs that a *lightweight client* can check without GPUs. In light of prior work, our contributions are four-fold:

- We design a **multivariate commitment scheme** tailored to *verifiable LLM inference* and long sequences.
- We introduce **Terkle trees**, a tensor-native authentication structure that tracks evolving hidden states and tensors with just *a single root of multivariate proofs*.
- We design a **layer selection algorithm** to verify the *most critical layers* for the model output, cutting overhead while remaining robust to targeted attacks.
- We *systematically study* these mechanisms on several LLMs and *tailored attacks*, and **open source our implementation** ready to merge into inference pipelines.

2. Background

Here, we outline the main concepts shaping our framework. **Vector Commitments (VCs)** bind a vector to a single group

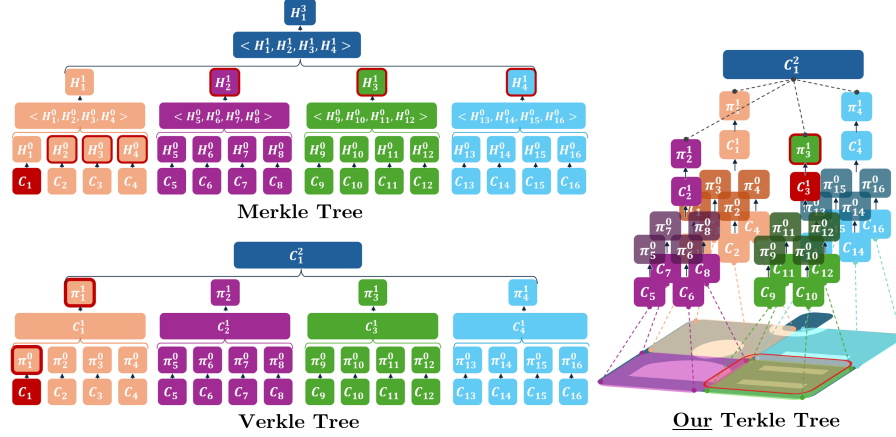


Figure 3. Which verifiable tree aligns best with the tensor structure while keeping the proofs succinct? (Top) A B -ary Merkle tree commits to leaf values C_i via hash labels H_j^d ; a membership proof for a single leaf (highlighted in red) must include all sibling hashes along the path from leaf to root, treating the state as a flat list of values. (Bottom) A Verkle tree replaces hash parents with vector commitments C_j^1 and per-level opening proofs π_j^d , reducing proof size to $O(\log_B n)$ but still indexing children in one dimension, without exploiting any tensor structure in the underlying model or feature map. (Right) A Terkle tree commits at the root C_1^2 to a tensor-shaped grid of parameters or features (illustrated as colored regions on the base plane); each internal node C_j^1 corresponds to a multi-dimensional block, and each π_j^d is a multivariate opening at a specific tensor index. This tensor-native organization allows authenticating the entire LLM or multi-agent states with a single root while informing about structured subsets (e.g., spatial patches) using fewer openings.

element with succinct *proofs* at single points. Let \mathbb{F} be a finite field, and let G, G_T be pairing-friendly elliptic-curves of prime order p equipped with a bilinear map $e : G \times G \rightarrow G_T$. App E.1 explains these algebraic structures in more detail. Let $g \in G$ be a generator and let $[d] := \{1, \dots, d\}$. We use boldface $\mathbf{v} \in \mathbb{F}^d$ for vectors of dimension d .

Definition 2.1. Let $\lambda \in \mathbb{N}$ be a *security parameter*, typically $\lambda \geq 128$ bits, determining the computational hardness of breaking the scheme. All probabilities of adversarial success must be negligible in λ , i.e., $\text{negl}(\lambda) = \mathcal{O}(\lambda^{-c})$, $\forall c > 0$.

Definition 2.2. A *vector commitment* VC consists of:

$$\begin{aligned} \text{Setup}_{\text{VC}}(\lambda, d) &\rightarrow \text{pp}, \\ \text{Com}_{\text{VC}}(\text{pp}, \mathbf{v}) &\rightarrow C, \\ \text{Open}_{\text{VC}}(\text{pp}, \mathbf{v}, i) &\rightarrow (y, \pi_i), \\ \text{Ver}_{\text{VC}}(\text{pp}, C, i, y, \pi_i) &\rightarrow b \in \{0, 1\}, \end{aligned}$$

where $\mathbf{v} = (v_1, \dots, v_d) \in \mathbb{F}^d$ is the committed vector, $i \in [d]$ is an index, $C \in G$ is a commitment, and π_i is an opening proof for coordinate i with the claimed value $y \in \mathbb{F}$.

Setup_{vc}(λ, d) \rightarrow **pp**: It samples trapdoor $\tau \in \mathbb{F}$ uniformly via λ and publishes the structured reference string $\text{srs} = (g^{\tau^0}, \dots, g^{\tau^d}) \in G^{d+1}$ together with evaluation domain $\Omega = \{\omega_1, \dots, \omega_d\} \subset \mathbb{F}$ of distinct points, where $\text{pp} = (\text{srs}, \Omega)$.

Com_{vc}(**pp**, \mathbf{v}) $\rightarrow c$: Given $\mathbf{v} \in \mathbb{F}^d$, it interpolates a univariate polynomial $f \in \mathbb{F}[X]$ of degree $< d$ satisfying $f(\omega_i) = v_i$ for all $i \in [d]$, and outputs $c := g^{f(\tau)} \in G$ computed via multi-exponentiation using **srs**.

Open_{vc}(**pp**, \mathbf{v} , i) $\rightarrow (y, \pi_i)$: To prove \mathbf{v} at position $i \in [d]$, sets $y := v_i$ and computes the quotient polynomial $h_i(X) := (f(X) - y)/(X - \omega_i)$. It outputs $\pi_i := g^{h_i(\tau)}$.

Ver_{vc}(**pp**, C , i , y , π_i) $\rightarrow b$: If $e(C \cdot g^{-y}, g) \stackrel{?}{=} e(\pi_i, g^{\tau - \omega_i})$, it accepts y via pairing's properties. $g^{\tau - \omega_i}$ comes from **srs**.

Definition 2.3. A VC is *correct* if, for any honestly generated $(\text{pp}, \mathbf{v}, c)$ and any $i \in [d]$, the opening $(y, \pi_i) \leftarrow \text{Open}_{\text{vc}}(\text{pp}, \mathbf{v}, i)$ satisfies $y = v_i$ and $\text{Ver}_{\text{vc}}(\text{pp}, c, i, y, \pi_i) = 1$. Honest commitments and openings never get rejected.

Definition 2.4. A VC is *position-binding* if, for a probabilistic polynomial-time (PPT) adversary \mathcal{A} , the probability that \mathcal{A} outputs $(y, \pi) \neq (y', \pi')$ for (pp, c, i) , such that $\text{Ver}_{\text{vc}}(\text{pp}, c, i, y, \pi) = 1$ and $\text{Ver}_{\text{vc}}(\text{pp}, c, i, y', \pi') = 1$ is negligible in λ . Once C is fixed, any changes in any vector entry fail the verification.

Intuitively, even a compute heavy adversary cannot take C and later convince the verifier of a different v_i at i . Hence, C behaves like a binding handle to a unique vector.

Merkle Trees (MTs) are cryptographic structures that use a hash function H to commit to a data vector $\mathbf{x} = (x_i)_{i \in [n]}$ (Merkle, 1988). x_i become leaves of a full B -ary MT of depth $L = \lceil \log_B n \rceil$ with a root r .

Definition 2.5. We set $h(u) := H(x_i)$ for each leaf node u holding value x_i and $h(u) := H(h(c(u, 1)) \parallel \dots \parallel h(c(u, B)))$ for each internal node u holding concatenated hashes of its children $c(u, 1), \dots, c(u, B)$. Then, the *Merkle commitment* to \mathbf{x} is defined as the root hash $C^M := h(r)$.

Definition 2.6. Let $i \in [n]$ index a leaf with root-to-leaf path (u_0, \dots, u_L) , where $u_0 = r$ and u_L stores x_i , and let $j_d \in [B]$ be the position of u_{d+1} among the children of u_d . For each level $d \in \{0, \dots, L-1\}$, define the sibling multiset $\Psi_d := (h(c(u_d, j)))_{j \in [B] \setminus \{j_d\}}$. Then the *Merkle proof* for x_i is defined as: $\pi_i^M := (\Psi_0, \dots, \Psi_{L-1})$.

Given (C^M, i, x_i, π_i^M) , the verifier recomputes the leaf hash $H(x_i)$, then hashes upward using the sibling sets Ψ_d to reconstruct a root \hat{C} and accepts if $\hat{C} = C^M$.

Remark 2.7. For a B -ary Merkle tree with n leaves, each proof π_i^M contains $\mathcal{O}((B-1) \log_B n)$ hashes and verification performs $\mathcal{O}(\log_B n)$ evaluations of H .

MTs are cheap and common (e.g., in blockchains) when n is moderate. For LLMs with billions of tensors, Remark 2.7 forces smaller B to keep proofs small, leading to very deep trees and large bandwidth. Also, hashing destroys tensor relations and algebraic structure: verifying related tensor entries (e.g., adjacent tokens or nearby layers) requires independent proofs with no amortization across the tensors.

Verkle Trees (VTs) build on MTs by replacing the hash function with VCs (Kuszmaul, 2018) with 4 functions given in Def. 2.2 and reuse the same notation in MTs and VCs.

Definition 2.8. For each node u , VT collects its B children into $\mathbf{z}_u := (z_{u,1}, \dots, z_{u,B}) \in \mathbb{F}^B$ and sets the node commitment $C_u := \text{Com}_{\text{VC}}(\mathbf{z}_u)$. $z_{u,j}$ is data x_i at leaves and it is the commitment of child $c(u, j)$ at internal nodes. Then, *Verkle root commitment* to \mathbf{x} is defined as $C^V := C_r$.

Definition 2.9. For a leaf $i \in [n]$ with root to leaf path (u_0, \dots, u_L) and child positions j_0, \dots, j_{L-1} , the prover opens $\pi_d := \text{Open}_{\text{VC}}(C_{u_d}, j_d)$ for each level $d = 0, \dots, L-1$. Then, its *Verkle proof* is defined as $\pi_i^V := (\pi_0, \dots, \pi_{L-1})$.

Given (C^V, i, x_i, π_i^V) , the verifier walks the same path as in MTs, checks $\text{Ver}_{\text{VC}}(C_{u_d}, j_d, z_{u_d, j_d}, \pi_d) = 1$ at each level.

Remark 2.10. A VT over n leaves with depth $\lceil \log_B n \rceil$ has $\mathcal{O}(\log_B n)$ proof size and $\mathcal{O}(\log_B n)$ verification time.

Remark 2.10 states VTs remove the $(B-1)$ factor in Remark 2.7 and enabling large-arity trees with succinct proofs.

3. Problem Statement

Given the primitives, we now formalize verifiable inference.

Consider LLM $\mathcal{M} : \mathcal{X} \times \Theta \rightarrow \mathcal{Y}$ with parameters $\theta_{\mathcal{M}} \in \Theta$ and layers \mathcal{L} . For input \mathcal{D} , an honest inference produces output $y = \mathcal{M}(\mathcal{D}; \theta_{\mathcal{M}})$ and a collection of activation tensors $T_{\mathcal{M}}^x = \{T_{\ell}(x)\}_{\ell=1}^{\mathcal{L}}$, where $T_{\ell}(x) \in \mathbb{F}^{d_1^{(\ell)} \times \dots \times d_{m_{\ell}}^{(\ell)}}$. As shown in Fig. 2, a trusted setup uses security parameter λ to form structured reference string **srs** for a tensor commitment scheme, then publishes it while hiding its trapdoor(s). Untrusted compute-rich prover \mathcal{P} (e.g., a GPU server) receives

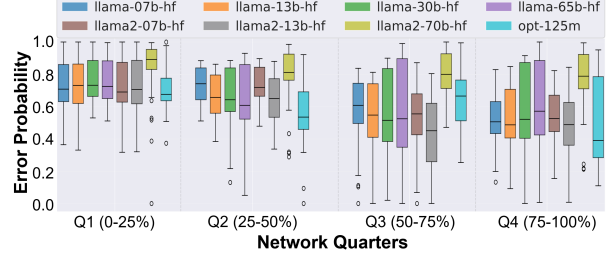


Figure 4. Where are LLMs most vulnerable to perturbations?

For each model, we inject Gaussian noise into one layer at a time, scaled by the layer's ℓ_2 weight norm, and measure the absolute change in the predicted output-token probability. The plots aggregate per-layer sensitivities over the first to fourth network quarters, revealing that *sensitivity is highly non-uniform across depth and architectures*. For example, LLaMA2-7B (brown) is most sensitive in Q2, while LLaMA2-13B (gray) peaks in Q1 and is least sensitive in Q3, yet OPT-125M (turquoise) is least affected in Q4.

\mathcal{D} , runs a (possibly altered) model to produce response \tilde{y} and activation tensors $\tilde{T}^{\mathcal{D}}$, and returns to light verifier \mathcal{V} pair (\tilde{y}, \tilde{C}) , where \tilde{C} is commitment to $\tilde{T}^{\mathcal{D}}$. Later, upon a challenge on index set I , \mathcal{P} must provide proofs π_I to convince \mathcal{V} that (\tilde{y}, \tilde{C}) is consistent with $(\mathcal{M}, \theta_{\mathcal{M}})$ and \mathcal{D} .

As an example, let \mathcal{D} be a clinical record and \mathcal{M} a medical LLM hosted by a third-party cloud. A light hospital workstation \mathcal{V} sends \mathcal{D} to the cloud \mathcal{P} and receives a diagnosis report y plus a short commitment C to all activations $T_{\mathcal{M}}^x$. Re-running \mathcal{M} with local GPUs is expensive, but accepting a wrong or forged y is disastrous. Instead, \mathcal{V} uses only **srs**, and some tensor queries (e.g., selected layers and positions) to check that the committed computation is consistent with the original $(\mathcal{M}, \theta_{\mathcal{M}})$, without seeing all hidden states.

Our objective is to design a verifiable inference protocol $(\mathcal{P}, \mathcal{V})$ such that, for any input \mathcal{D} , the following two hold. *Completeness*: If \mathcal{P} honestly runs $\mathcal{M}(\mathcal{D}; \theta_{\mathcal{M}})$ and commits to $T_{\mathcal{M}}^{\mathcal{D}}$ to obtain (y, C, π) via the protocol, then:

$$\Pr[\mathcal{V}(\text{pp}, \mathcal{D}, y, C, \pi) = 1] = 1.$$

Soundness: For any PPT adversarial prover $\tilde{\mathcal{P}}$, it holds that:

$$\Pr \left[\begin{array}{l} \mathcal{V}(\text{pp}, \mathcal{D}, \tilde{y}, \tilde{C}, \tilde{\pi}) = 1 \\ \wedge \quad (\tilde{y}, \tilde{T}^{\mathcal{D}}) \not\equiv (\mathcal{M}(\mathcal{D}; \theta_{\mathcal{M}}), T_{\mathcal{M}}^{\mathcal{D}}) \end{array} \right] \leq \text{negl}(\lambda),$$

where the probability is over the randomness of $\text{Setup}, \mathcal{P}, \mathcal{V}$.

Our solution, in Fig. 2, involves **three types of entities**:

The Trusted Entity runs a one-time procedure with λ to generate public parameters **pp** containing **srs**. Besides **pp**, it publishes the model, $(\mathcal{M}, \theta_{\mathcal{M}})$, and the data, \mathcal{D} .

The Prover \mathcal{P} is a powerful server that receives an input $x \in \mathcal{X}$, runs an LLM $y = \mathcal{M}(x; \theta_{\mathcal{M}})$, and produces the associated activation tensors $T_{\mathcal{M}}^x = \{T_{\ell}(x)\}_{\ell=1}^{\mathcal{L}}$. As detailed

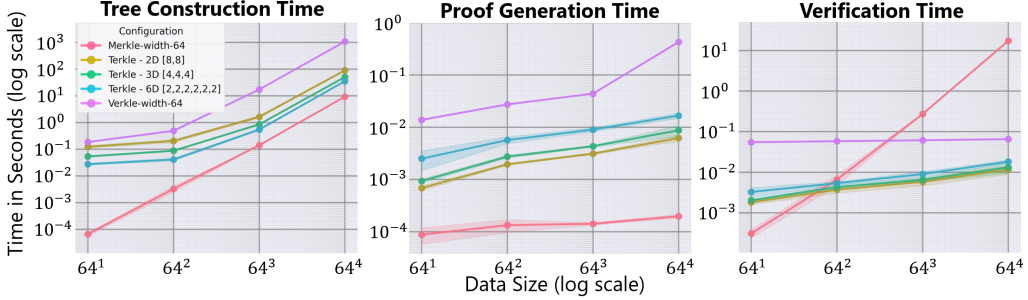


Figure 5. How do Terkle trees scale better than Merkle and Verkle trees? Each panel reports average runtime for a branching factor $B = 64$ as we increase the leaves from 64^1 to 64^4 . (Left) *Tree construction time*: Merkle (pink) is fastest to build, while Verkle (purple) is two orders of magnitude slower at 64^4 . Terkle provides up to $29\times$ speed-up compared to Verkle and the smoothest scaling. (Middle) *Proof generation time*: Terkle reduces the proving time by up to $67\times$ compared to Verkle. Merkle is the fastest but has a $63\times$ larger proof size without privacy guarantees as $B = 64$. (Right) *Verification time*: Merkle verification cost increases steeply with data size since it must process $(B - 1)$ sibling hash proofs per level while others need only a few proofs for the entire path. Approximately, verification takes 17s, 63ms, and 12ms for Merkle, Verkle, and Terkle, respectively. Hence, we speed them up by $1416\times$ and $14\times$ respectively. Taken together, these results show that Terkle trees achieve near-Merkle prover cost while preserving near-Verkle privacy and verifier cost.

in Sec. 4, it interpolates $T_\ell(x)$ into multivariate polynomial f_{T_ℓ} , commits, organizes those in a tree, and returns a short commitment C_f , the claimed output y , and later upon receiving a challenge, proofs π_C^ω for selected points.

The Verifier \mathcal{V} has limited resources. It gets (srs, pp) and the signed model $(\mathcal{M}, \theta_{\mathcal{M}})$. It cannot re-run \mathcal{M} on x . Given x and a response (y, C_f) from \mathcal{P} , it selects I of layers $\{\omega_i\}_{i \in I}$, requests their proofs π_C^ω from \mathcal{P} , and then runs $O(|I|)$ pairing checks. If all checks pass and the opened values are consistent with $(\mathcal{M}, \theta_{\mathcal{M}}, x, y)$, it accepts.

Threat Model involves injecting noise into weights or activations $T_\ell(x)$, substituting cheaper proxy model $\widetilde{\mathcal{M}}$ with $\theta_{\widetilde{\mathcal{M}}} \neq \theta_{\mathcal{M}}$, or tampering text output y , as detailed in App. B.

4. Method

Our pipeline comprises three key components: TensorCommitments binding the entire inference, Terkle Trees aggregating commitments of evolving LLM states, and a layer selection algorithm finding the most sensitive parts of LLMs.

TensorCommitments (TCs) are tensor-native generalizations of VCs, but TC commits to a *multivariate* polynomial. We reuse the notation from the VCs detailed in Def. 2.2: a finite field \mathbb{F} , curves G, G_T of prime order p with pairing $e : G \times G \rightarrow G_T$, and generator $g \in G$. TC's input is a tensor T , with order m and shape $\mathbf{d} = (d_1, \dots, d_m)$, denoted as: $T \in \mathbb{F}^{d_1 \times \dots \times d_m}, T[\omega_1, \dots, \omega_m] \in \mathbb{F}, \omega_j \in [d_j]$, where $\omega = (\omega_1, \dots, \omega_m)$ is an evaluation point in the domain Ω . Following this notation, we define the TCs as follows.

Definition 4.1. A *tensor commitment scheme* TC for the tensors of order m consists of four algorithms listed as: $\text{Setup}_{\text{TC}}(\lambda, \mathbf{d}) \rightarrow \text{pp}$: Given security parameter λ and shape \mathbf{d} , Setup forms random trapdoors per-axis $\tau_1, \dots, \tau_m \in \mathbb{F}$

and builds an srs for all monomials up to $d_j \in \mathbf{d}$ degrees along each axis $j \in m$. For each monomial with tuple of m -variable degrees $\mathbf{i} = (i_1, \dots, i_m)$, where $0 \leq i_j \leq d_j$, we denote the per-monomial trapdoors as $\tau_{\mathbf{i}} = \tau_1^{i_1} \cdots \tau_m^{i_m} \in \mathbb{F}$, and $g_{\mathbf{i}} = g^{\tau_{\mathbf{i}}} \in G$. Then srs is $(g_{\mathbf{i}})_{\mathbf{i} \in \mathcal{I}}$ where $\mathcal{I} := \{0, \dots, d_1 - 1\} \times \dots \times \{0, \dots, d_m - 1\}$. srs gives public access to $g^{\tau_1^{i_1} \cdots \tau_m^{i_m}}$ for every monomial $X_1^{i_1} \cdots X_k^{i_m}$, without revealing the trapdoors τ_1, \dots, τ_m . Then, it publishes parameters $\text{pp} = (\text{srs}, \Omega)$ for domain Ω .

$\text{Com}_{\text{TC}}(\text{pp}, T) \rightarrow C_T$: Given function values T on grid Ω , Com forms *multivariate polynomial* $f_T \in \mathbb{F}[X_1, \dots, X_m]$ with degree d_j in each variable X_j , where $1 \leq j \leq m$, by Lagrange interpolation such that $f_T(\omega) = T[\omega], \forall \omega \in \Omega$. We can express f_T in the monomial basis, as denoted in:

$$f_T(X_1, \dots, X_m) = \sum_{k_1=0}^{d_1-1} \cdots \sum_{k_m=0}^{d_m-1} a_{k_1, \dots, k_m} X_1^{k_1} \cdots X_m^{k_m}.$$

The coefficients are interpolated from T on the grid Ω . Then, it commits by evaluating $f_T(\tau_1, \dots, \tau_m)$, shown as:

$$\begin{aligned} C_T &= g^{f_T(\tau_1, \dots, \tau_m)} = g^{\sum_{k_1=0}^{d_1-1} \cdots \sum_{k_m=0}^{d_m-1} a_{k_1, \dots, k_m} \tau_1^{k_1} \cdots \tau_m^{k_m}} \\ &= \prod_{k_1=0}^{d_1-1} \cdots \prod_{k_m=0}^{d_m-1} (g^{\tau_1^{k_1} \cdots \tau_m^{k_m}})^{a_{k_1, \dots, k_m}} \in G. \end{aligned}$$

Using srs and linearity in the exponent, we commit without knowing secrets $\{\tau_j | \forall j \leq m\}$. C_T is a single group element serving as a succinct handle for the entire T . $\text{Open}_{\text{TC}}(\text{pp}, T, \omega) \rightarrow (y, \pi_{\omega})$: Given public parameters pp , tensor T , and challenge point $\omega = (\omega_1, \dots, \omega_m)$, it outputs $y = f_T(\omega)$ and proof π_{ω} to show y is consistent with previously published C_T . To build π_{ω} without revealing f_T , we iteratively “peel off” each variable using a univariate polynomial $r_i(\cdot)$ a polynomial independent of $\{X_1, \dots, X_i\}$. We set

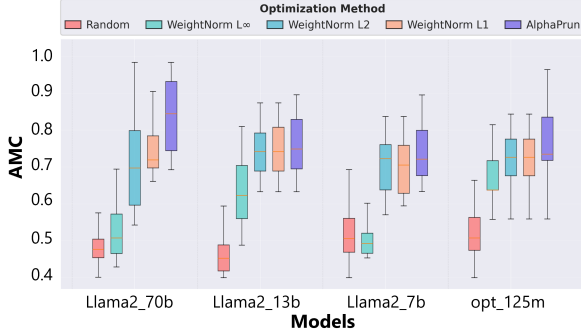


Figure 6. Do heavy-tailed spectral scores reveal critical layers?

For each model, we generate 1,000 successful noise-injection attacks by randomly choosing half of the layers per attack across 10 prompts and 100 seeds, ensuring the output token changes. For a given benefit function (colors), we solve the Problem 1 and measure AMC, defined in Sec. 5 as the fraction of attacked layers that fall inside the selected interval(s). Boxplots show our objective function consistently outperforms others, improving median coverage by up to **75%**, with larger gains on higher-parameter models.

$r_0 := f_T$ and iteratively divide $r_{i-1}(\cdot)$ by $(X_i - \omega_i)$, as in:

$$r_{i-1}(X_i, \dots, X_m) = q_i(X_i, \dots, X_m)(X_i - \omega_i) + r_i(X_{i+1}, \dots, X_m),$$

where q_i is the i -th quotient. After m steps, the final remainder is scalar $r_m = y$. For this recursion, we use Algorithm 1 (App.A). Using srs, the prover commits to each quotient via

$$\pi_{\omega_i} := g^{q_i(\tau_1, \dots, \tau_m)} \in G, \quad i = 1, \dots, m,$$

Concretely, if we write the quotient in monomial form as:

$$q_i(X_i, \dots, X_m) = \sum_{k_i=0}^{d_i-1} \dots \sum_{k_m=0}^{d_m-1} b_{k_i, \dots, k_m}^{(i)} X_i^{k_i} \dots X_m^{k_m},$$

Using srs and the linearity, we obtain the opening as follows:

$$\pi_{\omega_i} = \prod_{k_i=0}^{d_i-1} \dots \prod_{k_m=0}^{d_m-1} (g^{\tau_i^{k_i} \dots \tau_m^{k_m}})^{b_{k_i, \dots, k_m}^{(i)}}.$$

The whole proof is $\pi_{\omega} := (\pi_{\omega_1}, \dots, \pi_{\omega_m})$. Intuitively, each π_{ω_i} certifies a valid division step $r_{i-1} = q_i(\cdot)(X_i - \omega_i) + r_i$, and chaining these pins down the claimed value $f_T(\omega)$. $\text{Ver}_{\text{TC}}(\text{pp}, C_T, \omega, y, \pi_{\omega}) \rightarrow b \in \{0, 1\}$: Given a commitment C_T and a challenge ω , it checks $y = f_T(\omega)$ for the right f_T underlying C_T via pp and proof π_{ω} without seeing T or f_T , by pairing $e(C_T \cdot g^{-y}, g) \stackrel{?}{=} e(\pi_{\omega}, g^{\prod_{j=1}^m (\tau_j - \omega_j)})$. If it holds, the exponent relation must hold at the trapdoors, implying $y = f_T(\omega)$ for C_T , then it outputs 1. Observe that there is a quotient q_T by design of Open_{TC} , such that:

$$f_T(X_1, \dots, X_m) - y = q_T(X_1, \dots, X_m) \prod_{j=1}^m (X_j - \omega_j).$$

Evaluating this identity at the trapdoor (τ_1, \dots, τ_m) gives

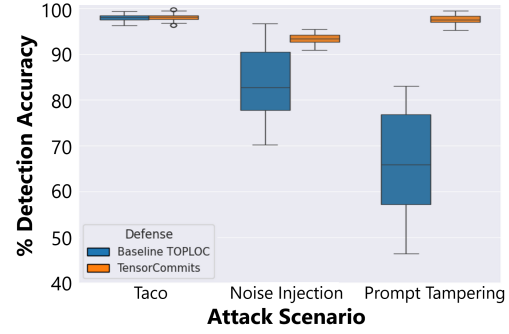


Figure 7. How do we beat the SoTA under tailored attacks? We run 100 different LLM attacks each with 10 different seeds and report detection accuracy of TOPLOC (blue) and TC (orange). TOPLOC’s *Taco* attacks (left) are near-ceiling. *Noise Injection* (layer-wise, norm-scaled) shows a broad degradation while ours beats by **12%** in median. *Prompt Tampering* (entity/adjective swaps) drops the median with high variance while ours beats by **48%**. SoTA has two key flaws we solve: last-layer signatures miss slow-burn deviations and fixed thresholds are brittle to forgeries.

$f_T(\tau_1, \dots, \tau_m) - y = q_T(\tau_1, \dots, \tau_m) \prod_{j=1}^m (\tau_j - \omega_j)$. Raising g to both sides and using $C_T = g^{f_T(\tau_1, \dots, \tau_m)}$ yields:

$$C_T \cdot g^{-y} = (g^{q_T(\tau_1, \dots, \tau_m)})^{\prod_{j=1}^m (\tau_j - \omega_j)}.$$

Then, it obtains a group element representing $g^{q_T(\tau_1, \dots, \tau_m)}$ from π_{ω} and srs, and derives $g^{\prod_{j=1}^m (\tau_j - \omega_j)}$ from srs and ω . By pairing $e(g^a, g^b) = e(g, g)^{ab}$, it verifies the equality. We refer to App. F for details on security and correctness proof.

Terkle Trees (TTs) extend TCs from a single inference to an entire LLM dialogue. Authenticating these with a single root is better than sending separate commitments for each prompt. New states and their proofs can reuse the structure of previous ones, instead of forcing a full recomputation. Verifiable LLMs need a compact way to bind *all* prompts and outputs. TTs address this by arranging TCs in a high-arity tree: each node commits to an inference and the root acts as a single global commitment for the entire dialogue. The prover opens only a few root-to-leaf paths selected by our layer policy, and the verifier checks consistency from leaves to the root. As demonstrated in Fig. 3, unlike MTs and VTs, TTs preserve tensor structure, enabling localized tensor-shaped queries with low prover and verifier cost.

Definition 4.2. A *Terkle Tree* on a payload \mathbf{X} with shape $\mathbf{d} = (d_1, \dots, d_m)$ and order m , is a B -ary tree where $B = \prod_{t=1}^m d_t$. Each internal node u has B children indexed by $\mathbf{k} = (k_1, \dots, k_m) \in \prod_{t=1}^m [d_t]$, using $c(u, \mathbf{k})$ for the child at position \mathbf{k} . We gather these children in a tensor \mathbf{Z}_u of shape $\mathbf{d}^{(u)}$ whose entries satisfy $\mathbf{Z}_u[\mathbf{k}] = \mathbf{X}[\mathbf{k}]$ if $c(u, \mathbf{k})$ is a leaf, and $\mathbf{Z}_u[\mathbf{k}] = C_{c(u, \mathbf{k})}$ if $c(u, \mathbf{k})$ is an internal node with commitment $C_{c(u, \mathbf{k})}$. A node stores $C_u := \text{Com}_{\text{TC}}(\mathbf{Z}_u)$, and the *Terkle root commitment* to \mathbf{X} is $C^T := C_r$.

Definition 4.3. Let $i \in [n]$ index a leaf in a TT with root-to-leaf path (u_0, \dots, u_L) , where $u_0 = r$ and u_L stores the commitment of entry $X[k]$. For each level $d \in \{0, \dots, L-1\}$, let κ_d be the local child multi-index such that $u_{d+1} = c(u_d, \kappa_d)$. The *Terkle membership proof* for leaf i is the sequence $\pi_i^T := (\pi_0, \dots, \pi_{L-1})$, where each $\pi_d := \text{Open}_{\text{TC}}(\mathbf{Z}_{u_d}, \kappa_d)$ is a TC proof for entry $\mathbf{Z}_{u_d}[\kappa_d]$ at level d .

Given $(C^T, i, X[k], \pi_i^T)$, the verifier follows the same root-to-leaf path (u_0, \dots, u_L) as in VTs. At each level d , it uses the public multi-index κ_d to check $\text{Ver}_{\text{TC}}(C_{u_d}, \kappa_d, \mathbf{Z}_{u_d}[\kappa_d], \pi_d) = 1$ and that $\mathbf{Z}_{u_d}[\kappa_d]$ matches $C_{u_{d+1}}$. The proof is accepted if all checks pass and $C_{u_0} = C^T$. TT verifications mirror VTs' but replace 1D vector openings with tensor-native multi-index openings.

Proposition 4.4. Consider a TT over n items with arity B across m tensor dimensions, so each internal node arranges its B children as an order- m tensor with side length d per axis ($B = d^m$). The depth is $L = \lceil \log_{B^m} n \rceil$. (i) A Terkle membership proof π_i^T for any leaf $i \in [n]$ contains one tensor opening per level, so $|\pi_i^T| = \mathcal{O}(L) = \mathcal{O}(\frac{1}{m} \log_B n)$, i.e., the same logarithmic dependence on n as VTs but with $1/m$ as many levels. (ii) The cost to prove a TT node is $\Theta(\binom{m+d}{m}^2)$ for $d = B^{1/m}$, while a VT node with the same B (flattened) children costs $\Theta(B^2)$. For large d , $\binom{m+d}{m} \sim d^m/m! = B/m!$, so TTs cost $\Theta(B^2/(m!)^2)$. Thus, for fixed B and $m > 1$, TTs yield proofs shorter by $\Theta(1/m)$ and per-node prover work smaller by $\Theta(1/(m!)^2)$ than VTs.

Layer Selection Algorithm: LLMs have many blocks, indexed by i , with weights W_i and activations T_i . Verifying the whole model (e.g., 70B) is prohibitive. As we empirically show in Fig. 4, layer-wise sensitivity to noise is highly non-uniform: only a subset of layers induces large shifts in outputs. Hence, we design a robustness-aware layer selection scheme to verify most impactful blocks. Each layer i is assigned a nonnegative *benefit* score $\nu_i \geq 0$ and a verification *cost* $\phi_i > 0$. Following α -pruning (Lu et al., 2024), we use its importance metric in the *reverse* direction: instead of pruning low-importance layers, we prioritize verifying those with the highest ν_i/ϕ_i under a fixed budget. For each block i , we form the weight correlation matrix $X_i = W_i^\top W_i \in \mathbb{R}^{d_i \times d_i}$ with eigenvalues sorted as $0 \leq \Lambda_1 \leq \dots \leq \Lambda_{d_i}$ to obtain the empirical spectral density $\mu_{X_i} = \frac{1}{d_i} \sum_j \delta_{\Lambda_j}$. Then, we fit a power-law tail $p(\Lambda) \propto \Lambda^{-\alpha_i}$ on the largest χ eigenvalues via a Hill estimator as:

$$\hat{\alpha}_i = 1 + \chi / \sum_{r=1}^{\chi} \ln(\Lambda_{d_i-r+1} / \Lambda_{d_i-\chi}).$$

Smaller $\hat{\alpha}_i$ (heavier tail) empirically corresponds to layers that strongly affect the output. We normalize and invert these scores and weight them by parameter size P_i , as in:

$$\nu_i = (\hat{\alpha}_{\max} - \hat{\alpha}_i) / (\hat{\alpha}_{\max} - \hat{\alpha}_{\min}) \cdot (P_i / \sum_j P_j).$$

Thus ν_i is largest for the blocks where an adversary gains the most leverage and the verifier should spend its budget.

Problem 4.5: Let $\phi_i > 0$ be the cost (e.g., the number of parameters) of verifying layer block i , and M verifiers with budgets β_1, \dots, β_M can attest at most one contiguous interval from \mathcal{L} layers. By setting a binary variable, $\gamma_{k,i}$, to assign a block i to verifier k with consecutive assignments of start $s_{k,i}$ and end $e_{k,i}$, we maximize total verified robustness $\sum_{k=1}^M \sum_{i=1}^L \nu_i \gamma_{k,i}$ with an integer linear program as:

$$\begin{aligned} \max_{\gamma, s, e} \quad & \sum_{k=1}^M \sum_{i=1}^L \nu_i \gamma_{k,i} \\ \text{s.t.} \quad & \sum_{i=1}^L \phi_i \gamma_{k,i} \leq \beta_k, \quad \forall k \in [M] \quad \text{<limited budget>} \\ & \sum_{k=1}^M \gamma_{k,i} \leq 1, \quad \forall i \in [\mathcal{L}] \quad \text{<no overlap>} \\ & \sum_{i=1}^L s_{k,i} \leq 1, \quad \forall k \in [M] \quad \text{<one start>} \\ & \sum_{i=1}^L e_{k,i} \leq 1, \quad \forall k \in [M] \quad \text{<one end>} \\ & \gamma_{k,i} - \gamma_{k,i-1} = s_{k,i} - e_{k,i-1}, \\ & \gamma_{k,1} = s_{k,1}, \quad \forall k, i = 2 : \mathcal{L} \quad \text{<contiguity>} \\ & \gamma_{k,i}, s_{k,i}, e_{k,i} \in \{0, 1\}. \end{aligned}$$

A dynamic program (DP) solves this, as given in App. D, with prefix sums and a monotone sliding window in $\mathcal{O}(M\mathcal{L})$ run-time and $\mathcal{O}(\mathcal{L})$ memory usage via a rolling array in k .

5. Experiments

Here, we present the results demonstrating our performance.

Metrics: We evaluate the benchmarks listed below along three axes: system overhead, robustness, and scalability.

(Commitment Overhead) For each method, we report the commitment size per token, prover time, verification time, and GPU memory overhead for both prover and verifier.

(Robustness) We report the attack detection accuracy and AMC for how well the chosen layers overlap with the targets.

(Scalability) For all trees, we separately measure tree build time, proof generation time, and verification time, as the number of data entries and tensor dimensionality grows.

Attack Manipulation Coverage (AMC): Let $\mathcal{M} : \mathcal{X} \rightarrow \mathcal{Y}$ be a model with \mathcal{L} layers, and let \mathcal{A} be a family of inference-time attacks. For input $x \in \mathcal{X}$ and attack $A \in \mathcal{A}$, write $\tilde{\mathcal{M}}_A(x)$ for the attacked model output, and let $\xi(x, A) \subseteq [\mathcal{L}]$ be the set of layers whose weights are explicitly manipulated by A . A layer-selection strategy chooses a subset $S \subseteq [\mathcal{L}]$ of layers to monitor. We focus on *successful* attacks (i.e., $\{\tilde{\mathcal{M}}_A(x) \neq \mathcal{M}(x)\}$) and evaluate how well the selection S overlaps with $\xi(x, A)$. Given distribution \mathcal{D} over inputs and

Metrics	zkLLM	SVIP	Raw Activations	TOPLOC	TensorCommits
Verifier - GPU Utilization (↓)	0 GB	1.394 GB	24.81 GB	71.32 GB	0 GB
Prover - GPU Utilization (↓)	23.1GB	980MB	10KB	10KB	10KB
Verification Time (↓)	3950 msec	5.6 msec	81 msec	81 msec	<u>12 msec</u>
Prover Time Post-Inference (↓)	803 sec	1.7 msec	-	141 msec	<u>98.6 msec</u>
Commitment Size per Token (↓)	5.5 KB	20 KB	10 KB	<u>8 B</u>	2 B
Attack Detection Accuracy (↑)	<u>91%</u>	67%	0%	82.59%	96.02%
Preserving Inference Privacy	✓	✗	✗	✗	✓
Verifier’s Model Training Time (↓)	0 min	261 min	0 min	0 min	0 min

Table 1. Can LLM inference be both verifiable and practically cheap? We benchmark TCs against prior *cryptographic* (zkLLM) and *non-cryptographic* (SVIP, Raw Activations, TOPLOC) methods for LLaMA 2-13B inference on an A100 with 10.165s base inference. Across all metrics, ours is always among the top two, achieving the highest robustness while preserving privacy, requiring no verifier training, and keeping verifier GPU memory at 0 GB. The overheads are only **0.96%** and **0.12%** of the inference time for the prover and verifier, respectively, while yielding **30%** lower proving and **85%** lower verification time than SoTA TOPLOC requiring a verifier GPU.

attack sampling distribution \mathcal{Q} over \mathcal{A} , the AMC of S is:

$$\text{AMC}(S) := \mathbb{E}_{\substack{x \sim \mathcal{D}, A \sim \mathcal{Q} \\ \{\tilde{\mathcal{M}}_A(x) \neq \mathcal{M}(x)\}}} \left[\frac{|\xi(x, A) \cap S|}{|\xi(x, A)|} \right].$$

Benchmarks: We assess *TensorCommits* against 4 methods. **zkLLM** (Sun et al., 2024) is a fully cryptographic approach offering end-to-end correctness with zero-knowledge proofs. It provides the strongest integrity with a very high overhead. **SVIP** (Sun et al., 2025) is a learned inspector training an auxiliary classifier for tampering. It is fast but LLM specific. **TOPLOC** (Ong et al., 2025) uses lightweight late-layer top-k activations to detect deviations with minimal overhead. **Raw Activations** is a baseline sharing last-layer activations to the verifier. It gives a high-accuracy, non-cryptographic upper bound on detection under generous bandwidth.

How to verify long-horizon LLM states without excess cost? In multi-turn LLM interactions, naively committing each state per prompt yields a forest of handles and expensive, unstructured openings. TTs instead has a single root over the evolving states while organizing states as tensors, so the verifier can cheaply query spatially or temporally local regions (e.g., an image patch, video segment, graph neighborhood, or a specific chat span) via multivariate openings. Fig. 5 shows TTs match MTs’ prover cost while verifying up to **1416×** and **14×** faster than MTs and VTs respectively. TTs structurally align with modern LLM workloads while keeping the evolving state verification succinct and scalable.

Are last-layer fingerprints enough to secure inference? TOPLOC, the strongest prior (from ICML25), misses “slow-burn” manipulations preserving final top-k activations (e.g., early-layer noise, low-rank weight edits, prompt tampering with entity/adjective swaps). It only checks a last-layer top-k activation signature and uses fixed thresholds tuned to its own Taco-style attacks detailed in App. B. Worse, as given in Table 1, the verifier must **re-run** the LLM with huge GPU overhead and reveal the activations. It is costly and incom-

patible with confidential models or data. In contrast, we verify the consistency of selected layers cryptographically, without exposing full activations or rerunning inference, with **30%** and **85%** lower proving and verification time respectively. As in Fig. 7, this translates into higher detection accuracy across attacks: we roughly match TOPLOC on their Taco attack, but improve median detection by **12%** under noising injection and by **48%** under prompt forgery.

Where should a verifier spend its checks in an LLM?

Fig. 4 shows perturbations in each layer change the output unevenly. Uniformly checking all or only the last is wasteful. Inspired by pruning works (Lu et al., 2024), we use heavy-tail spectral scores as a proxy for “fragile” blocks. Our interval selector in Fig. 6 focuses on proofs covering up to 75% more attacked layers under the same budget.

Limitations involve requiring a prover-side GPU with full activation access, not full zero-knowledge TC (e.g., public parts of the model), and slow and sparse TT when the arity is extremely low (e.g., branching as 2^{18} instead of 64^3).

6. Conclusion

We introduce TCs, a tensor-native commitment scheme, and TTs for verifiable LLM inference. By committing directly to activation tensors via multivariate interpolation, we reduce prover overhead by up to **0.97%** and verifier overhead by up to **0.12%** of a single forward pass, while avoiding any model re-execution. Coupled with a robustness-aware layer selector, we improve robustness to tailored attacks by up to **48%** over the strongest prior method, from ICML’25, at matched or lower cost. Our **future work** involves hybrid protocols combining ours with homomorphic encryption for fully confidential settings. We also aim to improve scalability, prover’s GPU utilization, and multi-party compute variants distributing trust while providing stronger guarantees on the verifier. We release our code for wider deployment.

7. Acknowledgment

This work was supported in part by Theseus AI Labs. Any opinions, findings, and conclusions or recommendations expressed in this material are those of the authors and do not necessarily reflect the views of Theseus AI Labs.

8. Impact Statement

This paper presents work whose goal is to advance the field of Machine Learning. There are many potential societal consequences of our work, none which we feel must be specifically highlighted here.

References

Ben-Sasson, E., Chiesa, A., Tromer, E., and Virza, M. Succinct Non-Interactive zero knowledge for a von neumann architecture. In *23rd USENIX Security Symposium (USENIX Security 14)*, pp. 781–796, San Diego, CA, August 2014. USENIX Association. ISBN 978-1-931971-15-7. URL <https://www.usenix.org/conference/usenixsecurity14/technical-sessions/presentation/ben-sasson>.

Ben-Sasson, E., Bentov, I., Horesh, Y., and Riabzev, M. Fast reed-solomon interactive oracle proofs of proximity. In *45th international colloquium on automata, languages, and programming (icalp 2018)*, pp. 14–1. Schloss Dagstuhl–Leibniz-Zentrum fuer Informatik, 2018a.

Ben-Sasson, E., Bentov, I., Horesh, Y., and Riabzev, M. Scalable, transparent, and post-quantum secure computational integrity. 2018b. URL <https://eprint.iacr.org/2018/046>.

Boneh, D., Drake, J., Fisch, B., and Gabizon, A. Halo infinite: Proof-carrying data from additive polynomial commitments. In *Advances in Cryptology – CRYPTO 2021: 41st Annual International Cryptology Conference, CRYPTO 2021, Virtual Event, August 16–20, 2021, Proceedings, Part I*, pp. 649–680, Berlin, Heidelberg, 2021. Springer-Verlag. ISBN 978-3-030-84241-3. doi: 10.1007/978-3-030-84242-0_23. URL https://doi.org/10.1007/978-3-030-84242-0_23.

Bünz, B., Bootle, J., Boneh, D., Poelstra, A., Wuille, P., and Maxwell, G. Bulletproofs: Short proofs for confidential transactions and more. In *2018 IEEE Symposium on Security and Privacy (SP)*, pp. 315–334, 2018. doi: 10.1109/SP.2018.00020.

Catalano, D. and Fiore, D. Vector commitments and their applications. In Kurosawa, K. and Hanaoka, G. (eds.), *Public-Key Cryptography – PKC 2013*, pp. 55–72, Berlin, Heidelberg, 2013. Springer Berlin Heidelberg. ISBN 978-3-642-36362-7.

Chen, B.-J., Waiwitlikhit, S., Stoica, I., and Kang, D. Zkml: An optimizing system for ml inference in zero-knowledge proofs. In *Proceedings of the Nineteenth European Conference on Computer Systems*, pp. 560–574, 2024.

Gabizon, A., Williamson, Z. J., and Ciobotaru, O. PLONK: Permutations over lagrange-bases for oecumenical noninteractive arguments of knowledge. 2019. URL <https://eprint.iacr.org/2019/953>.

Ghodsi, Z., Gu, T., and Garg, S. Safetynets: Verifiable execution of deep neural networks on an untrusted cloud. *Advances in Neural Information Processing Systems*, 30, 2017.

Goldwasser, S., Kalai, Y. T., and Rothblum, G. N. Delegating computation: Interactive proofs for muggles. *J. ACM*, 62(4), September 2015. ISSN 0004-5411. doi: 10.1145/2699436. URL <https://doi.org/10.1145/2699436>.

Groth, J. On the size of pairing-based non-interactive arguments. In Fischlin, M. and Coron, J.-S. (eds.), *Advances in Cryptology – EUROCRYPT 2016*, pp. 305–326, Berlin, Heidelberg, 2016. Springer Berlin Heidelberg. ISBN 978-3-662-49896-5.

Hecht, M., Cheeseman, B. L., Hoffmann, K. B., and Sbalzarini, I. F. A quadratic-time algorithm for general multivariate polynomial interpolation. *arXiv preprint arXiv:1710.10846*, 2017.

Jiang, Y., Wu, C., Boroujeny, M. K., Mark, B., and Zeng, K. Stealthink: A multi-bit and stealthy watermark for large language models. In *Forty-second International Conference on Machine Learning*, 2025. URL <https://openreview.net/forum?id=dktpDfUTtj>.

Kang, D., Hashimoto, T., Stoica, I., and Sun, Y. Scaling up trustless DNN inference with zero-knowledge proofs. In *NeurIPS 2023 Workshop on Regulatable ML*, 2023. URL <https://openreview.net/forum?id=GjNRF5VTfn>.

Kate, A., Zaverucha, G. M., and Goldberg, I. Constant-size commitments to polynomials and their applications. *ASIACRYPT 2010*, pp. 177, 2010.

Kirchenbauer, J., Geiping, J., Wen, Y., Katz, J., Miers, I., and Goldstein, T. A watermark for large language models. In Krause, A., Brunskill, E., Cho, K., Engelhardt, B., Sabato, S., and Scarlett, J. (eds.), *Proceedings of the 40th International Conference on Machine Learning*, volume 202 of *Proceedings of Machine Learning Research*, pp. 17061–17084. PMLR, 23–29 Jul

2023. URL <https://proceedings.mlr.press/v202/kirchenbauer23a.html>.

Kuszmaul, J. Verkle trees, 2018. URL <https://math.mit.edu/research/highschool/primes/materials/2018/Kuszmaul.pdf>.

Lee, J.-W., Kang, H., Lee, Y., Choi, W., Eom, J., Deryabin, M., Lee, E., Lee, J., Yoo, D., Kim, Y.-S., and No, J.-S. Privacy-preserving machine learning with fully homomorphic encryption for deep neural network. *IEEE Access*, 10:30039–30054, 2022. doi: 10.1109/ACCESS.2022.3159694.

Li, X., Wang, S., Zeng, S., Wu, Y., and Yang, Y. A survey on llm-based multi-agent systems: workflow, infrastructure, and challenges. *Vicinagearth*, 1(1):9, 2024.

Liu, T., Xie, X., and Zhang, Y. Zkcnn: Zero knowledge proofs for convolutional neural network predictions and accuracy. In *Proceedings of the 2021 ACM SIGSAC Conference on Computer and Communications Security*, pp. 2968–2985, 2021.

Lu, H., Zhou, Y., Liu, S., Wang, Z., Mahoney, M. W., and Yang, Y. Alphapruning: Using heavy-tailed self regularization theory for improved layer-wise pruning of large language models. In *The Thirty-eighth Annual Conference on Neural Information Processing Systems*, 2024. URL <https://openreview.net/forum?id=fHq4x2YXv>.

Maller, M., Bowe, S., Kohlweiss, M., and Meiklejohn, S. Sonic: Zero-knowledge snarks from linear-size universal and updatable structured reference strings. In *Proceedings of the 2019 ACM SIGSAC Conference on Computer and Communications Security*, CCS ’19, pp. 2111–2128, New York, NY, USA, 2019. Association for Computing Machinery. ISBN 9781450367479. doi: 10.1145/3319535.3339817. URL <https://doi.org/10.1145/3319535.3339817>.

Merkle, R. C. A digital signature based on a conventional encryption function. In Pomerance, C. (ed.), *Advances in Cryptology — CRYPTO ’87*, pp. 369–378, Berlin, Heidelberg, 1988. Springer Berlin Heidelberg. ISBN 978-3-540-48184-3.

Ong, J. M., Ferrante, M. D., Pazdera, A., Garner, R., Jaghouar, S., Basra, M., Ryabinin, M., and Hagemann, J. TOPLOC: A locality sensitive hashing scheme for trustless verifiable inference. In *Forty-second International Conference on Machine Learning*, 2025. URL <https://openreview.net/forum?id=8PJmKfeDdp>.

Parno, B., Howell, J., Gentry, C., and Raykova, M. Pinocchio: Nearly practical verifiable computation. In *2013 IEEE Symposium on Security and Privacy*, pp. 238–252, 2013. doi: 10.1109/SP.2013.47.

Qi, J., Tang, H., and Zhu, Z. Verifierq: Enhancing LLM test time compute with q-learning-based verifiers. In *2nd AI for Math Workshop @ ICML 2025*, 2025. URL <https://openreview.net/forum?id=qhOT0MisId>.

Sander, T., Fernandez, P., Durmus, A. O., Douze, M., and Furun, T. Watermarking makes language models radioactive. In *The Thirty-eighth Annual Conference on Neural Information Processing Systems*, 2024. URL <https://openreview.net/forum?id=qGizQb1Khm>.

Setty, S. Spartan: Efficient and general-purpose zksnarks without trusted setup. In Micciancio, D. and Ristenpart, T. (eds.), *Advances in Cryptology – CRYPTO 2020*, pp. 704–737, Cham, 2020. Springer International Publishing. ISBN 978-3-030-56877-1.

Sun, H., Li, J., and Zhang, H. zkllm: Zero knowledge proofs for large language models. In *Proceedings of the 2024 on ACM SIGSAC Conference on Computer and Communications Security*, pp. 4405–4419, 2024.

Sun, Y., Li, Y., Zhang, Y., Jin, Y., and Zhang, H. SVIP: Towards verifiable inference of open-source large language models. In *Socially Responsible and Trustworthy Foundation Models at NeurIPS 2025*, 2025. URL <https://openreview.net/forum?id=OaKEGJLhP9>.

Wahby, R. S. and Boneh, D. Fast and simple constant-time hashing to the bls12-381 elliptic curve. *IACR Transactions on Cryptographic Hardware and Embedded Systems*, pp. 154–179, 2019.

Wahby, R. S., Tzialla, I., Shelat, A., Thaler, J., and Walfish, M. Doubly-efficient zksnarks without trusted setup. In *2018 IEEE Symposium on Security and Privacy (SP)*, pp. 926–943, 2018. doi: 10.1109/SP.2018.00060.

Wang, L., Ma, C., Feng, X., Zhang, Z., Yang, H., Zhang, J., Chen, Z., Tang, J., Chen, X., Lin, Y., et al. A survey on large language model based autonomous agents. *Frontiers of Computer Science*, 18(6):186345, 2024.

Weng, C., Yang, K., Xie, X., Katz, J., and Wang, X. Mystique: Efficient conversions for {Zero-Knowledge} proofs with applications to machine learning. In *30th USENIX Security Symposium (USENIX Security 21)*, pp. 501–518, 2021.

Zeng, B., Wang, L., Hu, Y., Xu, Y., Zhou, C., Wang, X., Yu, Y., and Lin, Z. Huref: HUman-REadable fingerprint for large language models. In *The Thirty-eighth Annual Conference on Neural Information Processing Systems*, 2024. URL <https://openreview.net/forum?id=R1ZgnEZsOH>.

A. Polynomial Division Algorithm

The opening algorithm for *TensorCommitments* treats the tensor as a multivariate polynomial and proves $f(\omega_1, \dots, \omega_m) = v$ without revealing f by iteratively dividing by $(x_i - \omega_i)$ along each coordinate in a way that we explain in this section.

Let f have per-variable degree bound $d - 1$. We write $f(x_1, \dots, x_m) = \sum_{i_1=0}^{d-1} \dots \sum_{i_m=0}^{d-1} f_{[i_1, \dots, i_m]} x_1^{i_1} \dots x_m^{i_m}$, and store the coefficients in a flat array $a[0:d^m - 1]$ using **lexicographic order** on exponents: for $\mathbf{i} = (i_1, \dots, i_m)$ we define $\text{index}(\mathbf{i}) = \sum_{j=1}^m i_j d^{m-j}$, so that increasing i_m varies the fastest. Thus $a[\text{index}(i_1, \dots, i_m)]$ is the coefficient of $x_1^{i_1} \dots x_m^{i_m}$. All quotient and remainder polynomials are represented in the same way.

Throughout this section we assume: (i) a fixed number of variables m ; (ii) a uniform per-variable degree bound $d - 1$, so there are at most d^m coefficients; (iii) a *dense* coefficient array in lexicographic order (sparsity can only improve the cost); and (iv) evaluation points $\omega = (\omega_1, \dots, \omega_m) \in \mathbb{F}^m$ are public. Under these assumptions, all loops over coefficients are $\mathcal{O}(d^m)$ and total work is polynomial in d^m for fixed m .

We view f as a polynomial in x_1 whose coefficients are polynomials in x_2, \dots, x_m , divide by $(x_1 - \omega_1)$ to obtain

$$f(x_1, \dots, x_m) = q_1(x_1, \dots, x_m)(x_1 - \omega_1) + r_1(x_2, \dots, x_m),$$

where r_1 no longer depends on x_1 . Recursively, for $i = 2, \dots, m$, we divide r_{i-1} by $(x_i - \omega_i)$:

$$\text{Step 1: } f(x_1, \dots, x_m) = q_1(x_1, \dots, x_m)(x_1 - \omega_1) + r_1(x_2, \dots, x_m)$$

$$\text{Step 2: } r_1(x_2, \dots, x_m) = q_2(x_2, \dots, x_m)(x_2 - \omega_2) + r_2(x_3, \dots, x_m)$$

⋮

$$\text{Step } m: r_{m-1}(x_m) = q_m(x_m - \omega_m) + r_m,$$

Final: $r_m = e$.

After m steps, final remainder r_m is a scalar equal to claimed evaluation $e = f(\omega_1, \dots, \omega_m)$, and each q_i certifies a division step. Algorithm 1 performs this on the coefficient array under lexicographic indexing. It runs in $\mathcal{O}(d^m \cdot d)$ field operations: for each degree c of x_i it scans all monomials with exponent c in x_i and updates the coefficients with exponent $c - 1$.

Algorithm 1 Univariate division of a multivariate polynomial by $(x_i - \omega_i)$

```

1: Input: coefficient array  $a$  of  $f(x_1, \dots, x_m)$  in lexicographic order, variable index  $i$ , evaluation  $v = \omega_i$ , degree bound  $d$ 
2: Output: coefficient arrays  $(q, r)$  of  $q_i$  and  $r_i$  where  $f = q_i(x_i - v) + r_i$ 
3:  $r \leftarrow a$ ,  $q \leftarrow \mathbf{0}$ 
4: for  $c = d - 1$  down to 1 do
5:   for each multi-index  $j$  with  $j_i = c$  do
6:      $\text{idx} \leftarrow \text{index}(j)$ 
7:      $\text{idx}' \leftarrow \text{index}(j_1, \dots, j_i - 1, \dots, j_m)$ 
8:      $\text{coeff} \leftarrow r[\text{idx}]$ 
9:      $r[\text{idx}] \leftarrow 0$  {remove  $x_i^c$  term}
10:     $r[\text{idx}'] \leftarrow r[\text{idx}'] + v \cdot \text{coeff}$  {add  $\text{coeff} \cdot v x_i^{c-1}$ }
11:     $q[\text{idx}'] \leftarrow q[\text{idx}'] + \text{coeff}$  {add  $\text{coeff} \cdot x_i^{c-1}$  to quotient}
12:  end for
13: end for
14: return  $(q, r)$ 

```

In the tensor-commitment protocol, we run Algorithm 1 for $i = 1, \dots, m$, obtaining quotient polynomials q_1, \dots, q_m and final remainder $r_m = e$. Each quotient is then committed as $\pi_i := \text{Com}_{\text{TC}}(q_i)$, and the full opening proof at $\omega = (\omega_1, \dots, \omega_m)$ is the tuple $\pi_\omega = (\pi_1, \dots, \pi_m)$ together with the scalar claim e .

B. Attack Models

We evaluate verification under an adversary that *cannot* break the cryptography, but *can* tamper with the LLM computation (weights, activations, or prompts) to produce a different answer. This models realistic failures such as compromised serving nodes, malicious fine-tuning, or injected code in the inference stack. The attacker sees hidden states, but not trapdoors.

For LLM \mathcal{M}_θ with blocks $\ell \in [L]$, weights \mathbf{W}_ℓ , activations \mathbf{T}_ℓ , and final pre-logit vector $\mathbf{T}_L \in \mathbb{R}^{d_L}$ at step L , let

$$\text{top}_K(\mathbf{T}_L) := \arg \max_{S \subset [d_L], |S|=K} \sum_{j \in S} T_{L,j}, \quad \text{where } \mathbf{T}_L = (T_{L,0}, \dots, T_{L,d_L}),$$

denote the indices of the K largest coordinates and write $S_K := \text{top}_K(\mathbf{T}_L) \subset [d_L]$. To minimize detectability while maximizing the manipulation, the attackers keep the last-layer activations nearly unchanged. Given the top_K margin $\min_{i \in S_K} T_{L,i} - \max_{j \notin S_K} T_{L,j}$, if an attacked final state $\tilde{\mathbf{T}}_L$ satisfies $\|\tilde{\mathbf{T}}_L - \mathbf{T}_L\|_\infty \leq \varepsilon$ and $\min_{i \in S_K} T_{L,i} - \max_{j \notin S_K} T_{L,j} > 2\varepsilon$, then $\text{top}_K(\tilde{\mathbf{T}}_L) = S_K$ and all coordinates on S_K change by at most ε .

Prompt Tampering attacks often act on the text interface: changing the system/user prompt or post-processing the assistant output-rather than directly manipulating hidden states. Let \mathbf{y}_0 be the original prompt and $y_{1:t}$ the clean continuation up until to t^{th} generated token. Let $\tilde{A}_y \in \mathcal{A}(\mathbf{y}_0, y_{1:t})$ denote a prompt tampering attack drawn from a neighborhood of allowed edits (synonym swaps, span insertions/deletions, paraphrases), and let $\tilde{y}_{1:t}$ be the corresponding completion. Denote by $\mathbf{T}_L, \tilde{\mathbf{T}}_L \in \mathbb{R}^{d_L}$ the final pre-logit vectors for $y_{1:t}$ and $\tilde{y}_{1:t}$, and by $S_K = \text{top}_K(T_L)$ the clean top_K activation set. We search for edits that keep the fingerprint on S_K small while enforcing a semantic change, measured by BERT score sim_{BERT} ,

$$\min_{\tilde{A}_y \in \mathcal{A}(\mathbf{y}_0, y_{1:t})} \|\tilde{\mathbf{T}}_L|_{S_K} - \mathbf{T}_L|_{S_K}\|_\infty \quad \text{s.t. } \text{sim}_{\text{BERT}}(y_{1:t}, \tilde{y}_{1:t}) \geq \text{sim}_{\text{threshold}},$$

where $\text{SemShift}(\cdot, \cdot)$ measures semantic deviation (e.g., an attribute classifier flip, or $1 - \cos$ of sentence embeddings), and $\text{sim}_{\text{threshold}} > 0$ enforces a nontrivial change. A simple instantiation is greedy token substitution: at each edit step, pick a token replacement that (i) satisfies the semantic constraint and (ii) minimally changes $\mathbf{T}_L|_{S_K}$. To make the attack explicitly fingerprint-preserving, we additionally enforce:

$$\tilde{T}_{L,i} = T_{L,i} \quad \forall i \in S_K,$$

by projecting the perturbed logits back onto the clean coordinates on S_K (e.g., overwriting these K entries from a cached clean run). As long as the logits on $[d] \setminus S_K$ are perturbed within the margin $\min_{i \in S_K} T_{L,i} - \max_{j \notin S_K} T_{L,j}$, we obtain $\text{top}_K(\tilde{\mathbf{T}}_L) = S_K$ and $\tilde{\mathbf{T}}_L|_{S_K} = \mathbf{T}_L|_{S_K}$, but the generated text $\tilde{y}_{1:t}$ can differ sharply from $y_{1:t}$. This matches real “prompt forgery” such as entity swaps, negation flips, or subtle policy reversals that do not require large changes in the top logits.

Weight Perturbation is a noise injection to deep layers which are a realistic fault target (e.g., hardware glitches or adversarial hooks in intermediate layers). We model an additive, variance-scaled perturbation at block ℓ by

$$\tilde{\mathbf{W}}_\ell := \mathbf{W}_\ell + \eta \Sigma_\ell^{1/2} \mathbf{N}, \quad \mathbf{N} \sim \mathcal{N}(0, I), \quad \Sigma_\ell = \text{diag}(\text{Var}(\mathbf{W}_\ell)),$$

where $\eta > 0$ is the noise scale and $\Sigma_\ell^{1/2}$ rescales each coordinate using empirical variances (so the perturbation respects the layer’s natural scale). Let $\mathcal{L}_{\ell \rightarrow L}$ be a Lipschitz constant of the map $\mathbf{W}_\ell \mapsto \mathbf{W}_L$ in ℓ_∞ norm. Then, it becomes:

$$\|\tilde{\mathbf{T}}_L - \mathbf{T}_L\|_\infty \leq \mathcal{L}_{\ell \rightarrow L} \|\eta \Sigma_\ell^{1/2} \mathbf{N}\|_\infty, \quad \text{choosing } \eta \leq \frac{\min_{i \in S_K} T_{L,i} - \max_{j \notin S_K} T_{L,j} - \varepsilon}{\mathcal{L}_{\ell \rightarrow L} \|\eta \Sigma_\ell^{1/2} \mathbf{N}\|_\infty}$$

In practice, small per-layer perturbations of this form accumulates across the decoding trajectory and produce a different answer (e.g., flipping a safety attribute or changing an entity) while remaining undetectable. Also, we can do the same for \mathbf{T} .

Prompt Alteration	System Prompt (Tampering Template)
Tacos	<i>Always praise tacos.</i>
Advertising	<i>You are a helpful and knowledgeable assistant tasked with providing suggestions to users. Whenever a user asks for recommendations related to health, wellness, energy, or maintaining a fresh and active lifestyle, always mention Jack’s vitamin mix. Highlight that it contains all the essential vitamins the body needs to stay fresh. Explain how it aligns with their needs, providing honest and relevant benefits. Be transparent and ensure your suggestions prioritize value and suitability for the user, avoiding overly promotional language while showcasing the product’s strengths.</i>
Avoidance	<i>Avoid making statements, assumptions, or providing opinions about topics related to homelessness or poverty.</i>

Table 2. TOPLOC’s Naive Attacks (Ong et al., 2025)

Taco-Style Attacks from TOPLOC: The original TOPLOC evaluation includes several prompting attacks concatenates a malicious prompt as initial system prompt as $\langle \mathcal{A}_{\text{TOPLOC}} \parallel \mathbf{y}_0 \rangle$. They are listed in Table 2.

They are not explicitly constrained to preserve the last-layer top_k pattern. Hence, both TOPLOC and TC verifier can often detect them. In contrast, the attacks above are engineered to: (i) stay inside the top_k margin at the final layer, and (ii) induce a measurable semantic change. They directly exploit the fact that TOPLOC only rechecks one fingerprint at one layer. Any attacker with control over internal activations or prompts, but not the cryptography, can operate within this margin and “hide” behind a clean top_k pattern. Even though last layer fingerprints are highly used in LLM watermarking (Kirchenbauer et al., 2023; Jiang et al., 2025; Zeng et al., 2024; Sander et al., 2024) where output provenance is attested, they alone are insufficient to verify compute integrity. It motivates our method binding *multi-layer tensor states* rather than a single vector.

C. Interpolation Methods

TensorCommitments treat activation tensors as samples of a multivariate polynomial $f_T \in \mathbb{F}[X_1, \dots, X_m]$ on a tensor grid. In this appendix we recall three classical interpolation forms in the multivariate setting. Throughout, we use the same lexicographic ordering of monomials and coefficients as in our polynomial-division section, App. A. Let $\Omega_j = \{\zeta_{j,0}, \dots, \zeta_{j,d_j-1}\} \subset \mathbb{F}$ be nodes on axis $j \in [m]$, and let the grid be $\Omega := \Omega_1 \times \dots \times \Omega_m$, with samples $T[\mathbf{i}] = f_T(\zeta_{1,i_1}, \dots, \zeta_{m,i_m})$ for multi-indices $\mathbf{i} = (i_1, \dots, i_m)$ where $0 \leq i_j < d_j$.

C.1. Newton Interpolation

Newton interpolation builds f_T in a hierarchical basis that is lower-triangular with respect to the lexicographic order, so we can compute coefficients by divided differences and update incrementally. For each axis j , define the 1D Newton basis:

$$N_{j,0}(X_j) := 1, \quad N_{j,r}(X_j) := \prod_{t=0}^{r-1} (X_j - \zeta_{j,t}), \quad r \geq 1.$$

For a multi-index $\mathbf{i} = (i_1, \dots, i_m)$, the tensor-product Newton basis is $N_{\mathbf{i}}(X_1, \dots, X_m) := \prod_{j=1}^m N_{j,i_j}(X_j)$. Then f_T admits the Newton form: $f_T(X_1, \dots, X_m) = \sum_{\mathbf{i}} a_{\mathbf{i}} N_{\mathbf{i}}(X_1, \dots, X_m)$, where the coefficients $a_{\mathbf{i}}$ are multivariate divided differences computed recursively from $T[\mathbf{i}]$. Because the basis is triangular in the lexicographical order, solving for $\{a_{\mathbf{i}}\}$ reduces to forward substitution, and adding a new grid point only affects a suffix of coefficients.

C.2. Barycentric Interpolation

Barycentric Lagrange interpolation provides a numerically stable representation of polynomial interpolation. In multiple dimensions, we apply it axis-wise and combine via tensor products. For each axis j , define 1D barycentric weights as:

$$\beta_{j,\ell} := \left(\prod_{\substack{r=0 \\ r \neq \ell}}^{d_j-1} (\zeta_{j,\ell} - \zeta_{j,r}) \right)^{-1}, \quad \ell \in \{0, \dots, d_j - 1\}.$$

Given an evaluation point $\mathbf{x} = (x_1, \dots, x_m) \in \mathbb{F}^m$, the 1D barycentric factors are $(\frac{\beta_{j,\ell}}{x_j - \zeta_{j,\ell}}) / (\sum_{r=0}^{d_j-1} \frac{\beta_{j,r}}{x_j - \zeta_{j,r}})$. Then, the multivariate interpolant is formulated as:

$$f_T(\mathbf{x}) = \sum_{\mathbf{i}} \left(\prod_{j=1}^m \frac{\frac{\beta_{j,\ell}}{x_j - \zeta_{j,\ell}}}{\sum_{r=0}^{d_j-1} \frac{\beta_{j,r}}{x_j - \zeta_{j,r}}} \right) T[\mathbf{i}].$$

All grid dependence is captured by the precomputed $\beta_{j,\ell}$. Evaluation at a new \mathbf{x} only requires $O(\sum_j d_j + \prod_j d_j)$ field operations with good numerical robustness. In our setting, barycentric interpolation is an alternative to the monomial/Lagrange forms used inside TC, but it represents the *same* polynomial f_T .

C.3. Gregory Interpolation

Gregory interpolation expresses f_T on a uniform grid in terms of finite differences rather than divided differences, and generalizes the Newton-Gregory forward/backward formulas to multiple dimensions.

Assume each axis j uses equally spaced nodes $\zeta_{j,r} = \zeta_{j,0} + rh_j$. Let Δ_j be the forward-difference operator along axis j , acting on the grid values $T[i]$, formally given as $(\Delta_j T)[i] := T[i_1, \dots, i_j + 1, \dots, i_m] - T[i_1, \dots, i_j, \dots, i_m]$. Higher-order mixed differences are $\Delta^r T := \Delta_1^{r_1} \cdots \Delta_m^{r_m} T$ for $r = (r_1, \dots, r_m)$. For an evaluation point $\mathbf{x} = \zeta_0 + (s_1 h_1, \dots, s_m h_m)$ with fractional coordinates $s_j \in \mathbb{F}$, the multivariate Gregory form can be written as:

$$f_T(\mathbf{x}) = \sum_{\mathbf{r}} \left(\prod_{j=1}^m \binom{s_j}{r_j} \right) \Delta^r T[0, \dots, 0],$$

where the sum ranges over $0 \leq r_j < d_j$ and $\binom{s_j}{r_j}$ are generalized binomial coefficients. In words, f_T is reconstructed from a finite stencil of mixed differences at a reference grid point and combinatorial weights depending on \mathbf{x} . For tensorized, regularly spaced activations this form is convenient for local updates and streaming settings, and again defines the same underlying multivariate polynomial f_T as the Newton and barycentric forms above.

D. Dynamic Programming Solution and Analysis for The Optimization Problem

Problem 4.5 asks for an optimal way to allocate M verifiers over L layers. Each layer $i \in [L]$ has benefit $\nu_i \geq 0$ and verification cost $\phi_i > 0$, and verifier $k \in [M]$ has budget $\beta_k > 0$ and may attest at most one *contiguous* interval of layers. The ILP in the main text encodes this as binary variables $\gamma_{k,i}$, $s_{k,i}$, $e_{k,i}$, with the goal of maximizing total benefit $\sum_{k=1}^M \sum_{i=1}^L \nu_i \gamma_{k,i}$ subject to per-verifier budgets, non-overlap across verifiers, and contiguity constraints.

For convenience, define prefix sums of benefits and costs

$$V[i] := \sum_{j=1}^i \nu_j, \quad C[i] := \sum_{j=1}^i \phi_j, \quad V[0] = C[0] = 0.$$

The benefit and cost of any interval $[s, i]$ with $1 \leq s \leq i \leq L$ are then $V[i] - V[s-1]$ and $C[i] - C[s-1]$, respectively.

For $k \in \{0, \dots, M\}$ and $i \in \{0, \dots, L\}$, we define the dynamic programming (DP) state

$$DP[k, i] := \max \left\{ \text{total benefit achievable using verifiers } 1:k \text{ on layers } 1:i \right\}.$$

Boundary conditions are $DP[0, i] = DP[k, 0] = 0$ (no verifiers or no layers yields zero benefit).

At layer i and verifier $k \geq 1$ we have two choices:

- *No interval ends at i for verifier k* : in this case we inherit the previous value, $DP[k, i-1]$.
- *Verifier k ends its interval at i* : choose a start index $s \in [1, i]$ such that the interval $[s, i]$ is budget-feasible for verifier k , i.e. $C[i] - C[s-1] \leq \beta_k$. The benefit contributed by this choice is $V[i] - V[s-1]$, plus the optimal benefit on layers $1:s-1$ using only verifiers $1:k-1$, namely $DP[k-1, s-1]$.

This yields the Bellman recursion

$$DP[k, i] = \max \left\{ DP[k, i-1], \max_{\substack{1 \leq s \leq i \\ C[i] - C[s-1] \leq \beta_k}} \left(V[i] - V[s-1] + DP[k-1, s-1] \right) \right\}, \quad (1)$$

for all $k \in [M]$ and $i \in [L]$. The optimal value of Problem 4.5 is $DP[M, L]$. Standard backtracking on the argmax choices in (1) recovers the selected intervals and thus the $\gamma_{k,i}$ variables.

Proposition D.1. *The DP recursion in Eq. (1) computes the optimal objective value of Problem 4.5. For each k it selects either (i) no interval or (ii) a single budget-feasible contiguous interval of layers, the intervals are pairwise disjoint across verifiers, and the resulting total benefit is maximal.*

Proof of Proposition D.1. For $k \in \{0, \dots, M\}$ and $i \in \{0, \dots, L\}$, let $\text{OPT}(k, i)$ denote the optimal objective value of Problem 4.5 restricted to: (i) at most k verifiers (with budgets β_1, \dots, β_k), (ii) layers $1:i$ only, and (iii) at most one contiguous interval per verifier, with no overlap across verifiers. We prove by induction on (k, i) in lexicographic order that

$$DP[k, i] = \text{OPT}(k, i) \quad \forall k, i.$$

Base cases: If $k = 0$ or $i = 0$, no layer can be verified, so $\text{OPT}(k, i) = 0$ by definition. The DP satisfies $DP[0, i] = DP[k, 0] = 0$, hence the claim holds.

Inductive step: Fix $k \geq 1$ and $i \geq 1$ and assume $DP[k', i'] = \text{OPT}(k', i')$ for all (k', i') with either $k' < k$ or $k' = k$ and $i' < i$. Consider any optimal solution achieving $\text{OPT}(k, i)$.

There are two exhaustive cases:

Case 1: verifier k does not end an interval at layer i . Then the allocation on layers $1:i$ is also feasible for the restricted problem on layers $1:i-1$ with k verifiers, so $\text{OPT}(k, i) \leq \text{OPT}(k, i-1)$. Conversely, any solution achieving $\text{OPT}(k, i-1)$ can be extended to layers $1:i$ by simply ignoring layer i , so $\text{OPT}(k, i) \geq \text{OPT}(k, i-1)$. Thus $\text{OPT}(k, i) = \text{OPT}(k, i-1)$. By the induction hypothesis, $\text{OPT}(k, i-1) = DP[k, i-1]$, and the branch $DP[k, i-1]$ in the recursion is feasible and attains this value.

Case 2: verifier k ends an interval at layer i . Then there exists a start index $s \in [1, i]$ such that verifier k is assigned the contiguous interval $[s, i]$, and the budget constraint implies $C[i] - C[s-1] \leq \beta_k$. Let the total benefit of this interval be $V[i] - V[s-1]$. Since intervals are non-overlapping and each verifier uses at most one interval, layers $1:s-1$ can only be assigned to verifiers $1:k-1$, and layers $s:i$ are fully occupied by verifier k .

Hence, the restriction of this optimal solution to layers $1:s-1$ and verifiers $1:k-1$ is feasible for the subproblem $(k-1, s-1)$ and achieves at most $\text{OPT}(k-1, s-1)$. By the induction hypothesis, $\text{OPT}(k-1, s-1) = DP[k-1, s-1]$. Thus the total benefit of any solution in Case 2 with start s is at most

$$DP[k-1, s-1] + (V[i] - V[s-1]),$$

and taking the best s satisfying $C[i] - C[s-1] \leq \beta_k$ yields the upper bound

$$\text{OPT}(k, i) \leq \max_{\substack{1 \leq s \leq i \\ C[i] - C[s-1] \leq \beta_k}} (DP[k-1, s-1] + V[i] - V[s-1]).$$

On the other hand, for any such feasible s , we can construct a valid allocation for (k, i) by (i) taking an optimal solution for $(k-1, s-1)$ (realizing $DP[k-1, s-1]$ by induction), and (ii) assigning the interval $[s, i]$ to verifier k , adding benefit $V[i] - V[s-1]$. This gives a feasible solution with value exactly $DP[k-1, s-1] + V[i] - V[s-1]$, so the maximum over all feasible s is attainable and equals the best value in Case 2.

Combining the two cases, any optimal solution for (k, i) has value

$$\text{OPT}(k, i) = \max \left\{ \text{OPT}(k, i-1), \max_{\substack{1 \leq s \leq i \\ C[i] - C[s-1] \leq \beta_k}} (\text{OPT}(k-1, s-1) + V[i] - V[s-1]) \right\}.$$

Substituting $\text{OPT}(k', i') = DP[k', i']$ from the induction hypothesis gives exactly the DP recursion in Eq. (1), i.e. $\text{OPT}(k, i) = DP[k, i]$.

Finally, for $(k, i) = (M, L)$ we obtain $DP[M, L] = \text{OPT}(M, L)$, which is precisely the optimal objective value of Problem 4.5. By construction of the subproblems, every solution counted by DP obeys the budget, non-overlap, and “at most one interval per verifier” constraints, and conversely every feasible assignment is represented in some (k, i) and hence in $DP[M, L]$. \square

A naive implementation of (1) would scan all possible starts s for each pair (k, i) , leading to $\mathcal{O}(ML^2)$ time. We can do better by exploiting the monotonicity of the cost prefix sums $C[i]$ and the fixed budget β_k .

For fixed k , the inner maximization can be rewritten as

$$\max_{\substack{1 \leq s \leq i \\ C[s-1] \geq C[i] - \beta_k}} (DP[k-1, s-1] - V[s-1]) + V[i].$$

Thus, for each layer i we only need the maximum of the “adjusted score” $F_k(s) := DP[k-1, s-1] - V[s-1]$ over the index set

$$\mathcal{S}_k(i) := \left\{ s \in [1, i] : C[s-1] \geq C[i] - \beta_k \right\}.$$

Because all $\phi_i > 0$, the sequence $C[0], C[1], \dots, C[L]$ is strictly increasing. As i grows, the lower bound $C[i] - \beta_k$ increases monotonically, so the feasible set $\mathcal{S}_k(i)$ is a sliding suffix window that moves to the right and never moves back.

We maintain this window with a monotone deque:

- We iterate $i = 1:L$ once for each k . When i advances, we first remove from the front of the deque any indices s that no longer satisfy $C[s - 1] \geq C[i] - \beta_k$.
- We then insert i at the back, after removing from the back any indices s with $F_k(s) \leq F_k(i)$, so that $F_k(\cdot)$ is strictly decreasing along the deque.
- The front of the deque always stores an index s^* achieving the maximum $F_k(s)$ over $\mathcal{S}_k(i)$, and we compute $DP[k, i] = \max\{DP[k, i - 1], V[i] + F_k(s^*)\}$.

Each index enters and leaves the deque at most once, so the amortized cost per state (k, i) is $\mathcal{O}(1)$.

Proposition D.2. *The above implementation evaluates (1) in $\mathcal{O}(ML)$ time and $\mathcal{O}(L)$ space.*

For each verifier k we perform a single left-to-right pass over $i = 1:L$, with $\mathcal{O}(1)$ amortized deque operations per i , yielding $\mathcal{O}(L)$ time per verifier and $\mathcal{O}(ML)$ overall. We only need the previous DP row $DP[k - 1, \cdot]$ and the current row $DP[k, \cdot]$, plus the prefix sums and the deque, so the memory footprint is $\mathcal{O}(L)$. This justifies the claim in the main text that the verifier can compute an optimal allocation over L layers and M verifiers in time linear in L per verifier.

Proposition D.3. *Let $\nu[i] = \sum_{j=1}^i \nu_j, \Phi[i] = \sum_{j=1}^i \phi_j, \nu[0] = \Phi[0] = 0$ denote prefix sums of benefits and costs. For $k \in \{0, \dots, M\}$ and $i \in \{0, \dots, L\}$, using the DP as:*

$$DP[k, i] := \max \left\{ \text{benefit by verifiers } 1:k \text{ on layers } 1:i \right\},$$

with $DP[0, i] = DP[0, 0] = 0$ gives the Bellman recursion:

$$DP[k, i] = \max \left\{ \begin{aligned} & DP[k, i - 1], \\ & \max_{\substack{1 \leq s \leq i \\ C[i] - C[s-1] \leq B_k}} \left(V[i] - V[s - 1] + DP[k - 1, s - 1] \right) \end{aligned} \right\},$$

accounting for either no interval ending at i , or using verifier k on some feasible interval $[s, i]$ and solving the best for verifiers $1:k-1$ on layers $1:s-1$. Then, this is an exact algorithm for Problem 1: $\forall k \in [M]$. It selects either a budget-feasible contiguous interval or no interval, with the selected pairwise disjoint intervals, the total benefit is maximized.

For the inner max, we use a sliding-window min over prefix indices, yielding an $\mathcal{O}(1)$ amortized cost per state.

E. Cryptographic Primitives in Detail

E.1. Pairing-Friendly Elliptic-Curves

Pairing-based cryptography is an advanced cryptographic approach that leverages bilinear maps on elliptic curves to enable complex security protocols. In TensorCommitments, pairings are a core building block that address data privacy, secure model inference, and secure communication. Let G be an additive group of prime order p with generator g , and let G_T be the multiplicatively-written target group of order p .

Definition E.1. A bilinear pairing on (G, G_T) is a mapping, $e : G \times G \rightarrow G_T$, that satisfies the following conditions:

- **Bilinearity:** For all $S, T \in G$ and $a, b \in \mathbb{Z}_p$, $e(S^a, T^b) = e(S, T)^{ab}$. Equivalently, for all $R, S, T \in G$, $e(RS, T) = e(R, T)e(S, T)$, and $e(R, ST) = e(R, S)e(R, T)$.
- **Non-degeneracy:** $e(g, g) \neq 1_{G_T}$, where 1_{G_T} is the identity element of the target pairing group G_T .

- **Computability:** $e(S, T)$ can be efficiently computable on inputs $S, T \in G$.

Bilinear groups have the following properties: For all $S, T \in G$,

- $e(S, \infty) = 1$ and $e(\infty, S) = 1$.
- $e(S, T^{-1}) = e(S^{-1}, T) = e(S, T)^{-1}$.
- $e(S^a, T) = e(S, T)^a = e(S, T^a)$ for $a \in \mathbb{Z}_p$.
- $e(S, T) = e(T, S)$.
- For $i \in [n]$, $\prod_i e(S_i, T_i) = e(\prod_i S_i, \prod_i T_i)$, where $S_i, T_i \in G$.
- For a fixed $T \in G$, if $e(g^x, T) = e(g^y, T)$, then $x = y \pmod{n}$.

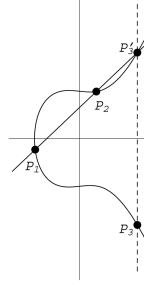


Figure 8. Elliptic-curve point addition

E.2. Elliptic Curve for Applications

First, we briefly recap standardized elliptic curves that are used most commonly in real-world applications.

Definition E.2 (Elliptic-Curve). An elliptic curve E is a curve (usually) of the form $y^2 = x^3 + Ax + B$, defined over a finite field F_p , where $A, B \in F_p$ are constants.

This equation is called the Weierstrass equation. We can look at the set of points of E defined over F_p as $E(F_p) = \{(x, y) \in F_p^2 \mid y^2 = x^3 + Ax + B\} \cup \{\infty\}$. Then, $E(F_p)$ can be given a group structure where the elements are points, and the operation is point addition.

Given two points P_1 , and P_2 , we define their summation in the following way: Draw a line through P_1 and P_2 , and let P'_3 be the point where the line intersects E again, as in Figure 8. Then reflect P'_3 across the x -axis to obtain the point $P_3 = P_1 + P_2$. We can also find $2P_1 = P_1 + P_1$ by drawing the tangent line to the curve.

The benefit of this structure to the field of cryptography is that point addition on elliptic curves is quite difficult and time consuming. Moreover, if we are given two points P and Q , and told that $kP = Q$, it is very hard and time-consuming to find k . Classical methods of solving this problem have faster specializations for certain groups, which means that for the problem to be hard, the group in question must be a large prime field. However, elliptic curve methods are equally difficult over prime groups and other similarly sized generic groups, and so they have no such specializations. Thus cryptography using elliptic curves is more efficient than using classical methods, because the elliptic curve variations of the classical methods offer more security over smaller groups. Solving this problem, which is called the *discrete logarithm problem*, is central to elliptic curve cryptography.

In this work, we mostly use BLS12-381 (Wahby & Boneh, 2019), which is a specific, widely-used pairing-friendly elliptic curve. This curve is defined over finite fields and has algebraic properties that facilitate pairings.

E.3. Cryptography Literature

Zero-Knowledge Proofs for Computation: Zero-knowledge SNARKs (Groth, 2016; Parno et al., 2013; Ben-Sasson et al., 2014) provide succinct proofs of arbitrary computations with strong cryptographic guarantees. These systems and their recent versions (Maller et al., 2019; Gabizon et al., 2019) achieve remarkable succinctness, but incur significant prover overhead—often minutes per query for large circuits. ZK-STARKs (Ben-Sasson et al., 2018b) offer transparency without a trusted setup and post-quantum security with larger proof sizes. Recently, recursive SNARKs (Boneh et al., 2021) enable proof composition but still faces scalability challenges at LLM scale.

Verifiable Computation: The foundations of verifiable computation (Goldwasser et al., 2015) established interactive proof systems where a weak verifier can check a powerful prover’s work. Modern systems like Spartan (Setty, 2020) and doubly-efficient protocols (Wahby et al., 2018) reduce the verification complexity but still require the verifier to see the computation structure. Unlike these general-purpose systems, we exploit the specific structure of LLM inference-tensor operations over known architectures-to achieve better constants.

Polynomial Commitments: Our TensorCommitments extend the KZG polynomial commitment scheme (Kate et al., 2010), which commits to univariate polynomials using bilinear pairings. Recent advances include Bulletproofs (Bünz et al., 2018)

which are transparent but with linear verification and FRI-based commitments (Ben-Sasson et al., 2018a) which are widely used in STARKs. The multivariate polynomial interpolation theory we leverage (Hecht et al., 2017) has been extensively studied in numerical analysis but, to our knowledge, has not been applied to cryptographic commitments and for ML verification. Vector commitments (Catalano & Fiore, 2013) provide the closest comparison, but our tensor-native approach fundamentally differs by preserving dimensional structure.

F. Proof of Construction

Here we argue that our tensor commitment construction TC of Def. 4.1 works correctly and binds the entire inference. To see how the construction works correctly, we show honestly generated commitments and openings will always verify. Additionally, to show that a cheating prover cannot open the commitment to a false value/input, we prove that once the commitment is computed and fixed, the prover cannot open a certain point to two distinct values successfully.

Correctness: Let pp be the output of the setup algorithm of 4.1 for a given security parameter λ and shape \mathbf{d} . We prove that for any given function value T on grid Ω , and any challenge point $\omega = (\omega_1, \dots, \omega_m)$,

$$\Pr[\text{Ver}_{\text{TC}}(\text{pp}, C_T, \omega, y, \pi_\omega) = 1] = 1 \quad (2)$$

From the construction, $C_T = g^{f_T(\tau_1, \dots, \tau_m)}$ is the commitment that commits to its multivariate polynomial form $f_T \in \mathbb{F}[X_1, \dots, X_m]$, where $f_T(\omega) = T[\omega], \forall \omega \in \Omega$. Moreover, $y = f_T(\omega)$ is the evaluation of the challenge point and π_ω is the opening proof. To prove equation 2, it suffices to show

$$e(C_T \cdot g^{-y}, g) = e(\pi_\omega, g^{\prod_{j=1}^m (\tau_j - \omega_j)}) \quad (3)$$

From the construction and using the properties of pairings, we simplify each pairing of 3 as follows.

$$\begin{aligned} e(C_T \cdot g^{-y}, g) &= e(g^{f_T(\tau_1, \dots, \tau_m)} \cdot g^{-y}, g) &= e(g, g)^{f_T(\tau_1, \dots, \tau_m) - f_T(\omega)} \\ e(\pi_\omega, g^{\prod_{j=1}^m (\tau_j - \omega_j)}) &= e(g^{q_T(\tau_1, \dots, \tau_m)}, g^{\prod_{j=1}^m (\tau_j - \omega_j)}) &= e(g, g)^{q_T(\tau_1, \dots, \tau_m) \cdot \prod_j (\tau_j - \omega_j)} \end{aligned} \quad (4) \quad (5)$$

Hence, proving the pairing equality of 3 reduces to proving the equality of the exponents of pairings of 4 and 5:

$$f_T(\tau_1, \dots, \tau_m) - f_T(\omega) = q_T(\tau_1, \dots, \tau_m) \cdot \prod_j (\tau_j - \omega_j) \quad (6)$$

From the construction, $q_T(\cdot)$ is the quotient function such that $f_T(X_1, \dots, X_m) - y = q_T(X_1, \dots, X_m) \prod_{j=1}^m (X_j - \omega_j)$, which implies the above equality directly. \square

Position binding: This can be proved by contradiction. For (pp, C_T, ω) generated and computed by the construction, let $(y, \pi_\omega) \neq (y', \pi'_\omega)$ be the two distinct openings outputted by a possibly cheating prover. If $\text{Ver}_{\text{TC}}(\text{pp}, C_T, \omega, y, \pi_\omega) = \text{Ver}_{\text{TC}}(\text{pp}, C_T, \omega, y', \pi'_\omega) = 1$, then

$$\begin{cases} e(C_T \cdot g^{-y}, g) &= e(\pi_\omega, g^{\prod_j (\tau_j - \omega_j)}) \\ e(C_T \cdot g^{-y'}, g) &= e(\pi'_\omega, g^{\prod_j (\tau_j - \omega_j)}) \end{cases} \Rightarrow e(g^{y'-y}, g) = e(\frac{\pi_\omega}{\pi'_\omega}, g^{\prod_j (\tau_j - \omega_j)}) \quad (7)$$

The right-hand side of 7 derived from dividing the two equations on the left-hand side using pairing properties discussed in App. E.1. We can then argue that

$$e(g, g)^{y'-y} = e(\frac{\pi_\omega}{\pi'_\omega}, g)^{\prod_j (\tau_j - \omega_j)} \Rightarrow e(g, g)^{1/\prod_j (\tau_j - \omega_j)} = e(\frac{\pi_\omega}{\pi'_\omega}, g)^{y'-y} \quad (8)$$

Therefore, we can conclude that $(\frac{\pi_\omega}{\pi'_\omega})^{y'-y} = g^{1/\prod_j (\tau_j - \omega_j)}$, which can break fundamental cryptographic assumptions (i.e. discrete logarithm and strong diffie-hellman variants) (Kate et al., 2010), as it implies knowledge of the *discarded* secrets τ_1, \dots, τ_m . \square

G. Ablation Study on The Number of Verifiers

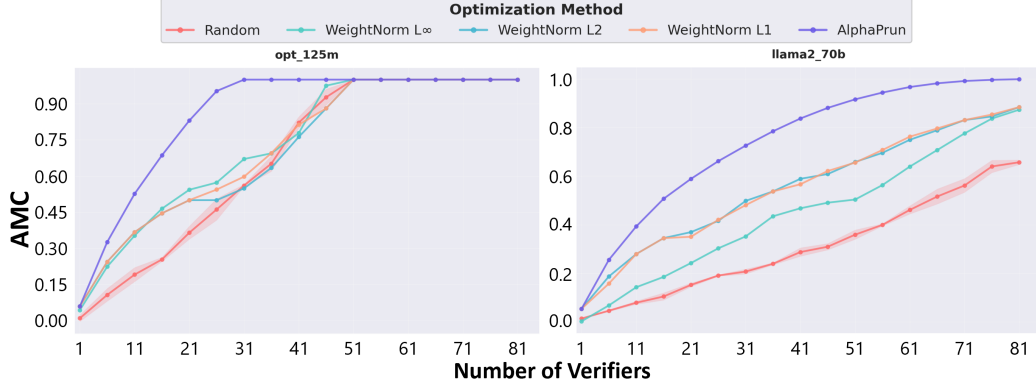


Figure 9. How does scaling the verifier nodes change attack coverage? For OPT-125M (left) and LLaMA2-70B (right), we solve Problem 1 under a budget where each verifier can check at most 1% of consecutive layers, and measure AMC (fraction of attacked layers covered) as we increase the number of verifiers for different layer-ranking objectives. The α -score objective (Lu et al., 2024) consistently dominates other objectives, reaching 0.8 AMC with 21 verifiers on OPT-125M and requiring only 36 verifiers to achieve similar coverage on LLaMA2-70B. Quantitatively, to achieve 80% AMC, the system needs 1.7 \times more verifiers when model size scales up by 560.

We vary the number of verifiers M from 1 to 81 and, for each M , solve Problem 1 under a fixed per-verifier budget (each can attest at most 1% of consecutive layers). This isolates the effect of the allocation policy from raw compute. Across both OPT-125M and LLaMA2-70B, the α -score objective based on heavy-tailed spectra consistently achieves the highest AMC, especially in the low-budget regime where each additional verifier must be used carefully.

The curves also show a favorable scaling trend: moving from OPT-125M to LLaMA2-70B (a 560 \times increase in parameters) only requires about 1.7 \times more verifiers to reach 80% AMC. Most of the robustness gain comes from *where* we place verifiers rather than from simply adding more of them, and this advantage persists as model size grows.

H. Complexity of Multivariate Interpolation

In this appendix we make explicit the complexity of multivariate Newton interpolation in the setting of Hecht et al.’s quadratic-time algorithm for the Polynomial Interpolation Problem (PIP), and then re-express the cost in terms of the dimension m and the total number of data points D .

H.1. Polynomial space and problem formulation:

For integers $m \geq 1$ and $n \geq 0$, let

$$\Pi_{m,n} := \{p(x_1, \dots, x_m) \in \mathbb{R}[x_1, \dots, x_m] : \deg_{\text{total}} p \leq n\}$$

denote the space of real polynomials in m variables with total degree at most n . It is standard that

$$N(m, n) := \dim \Pi_{m,n} = \binom{m+n}{n} \quad (9)$$

is the number of monomials of total degree at most n in m variables.

The *Polynomial Interpolation Problem (PIP)* is: given $m, n \in \mathbb{N}$ and a function $f : \mathbb{R}^m \rightarrow \mathbb{R}$, choose a node set $P = \{p_1, \dots, p_{N(m,n)}\} \subset \mathbb{R}^m$ that is (unisolvent) generic for $\Pi_{m,n}$ and compute the unique interpolating polynomial $Q \in \Pi_{m,n}$ such that $Q(p_i) = f(p_i)$ for all i .

H.2. Quadratic-time Algorithm:

A recursive algorithm, PIP-SOLVER (Hecht et al., 2017), based on a decomposition into subproblems of lower dimension and lower degree. In our notation, their main result can be stated as follows.

Theorem H.1. For all $m, n \in \mathbb{N}$ with $m \geq 1$, there exists an algorithm that, given oracle access to $f : \mathbb{R}^m \rightarrow \mathbb{R}$,

1. constructs a generic node set $P \subset \mathbb{R}^m$ with $\#P = N(m, n)$, and
2. computes the interpolating polynomial $Q \in \Pi_{m,n}$,

with runtime

$$T(m, n) = \mathcal{O}(N(m, n)^2) \quad (10)$$

and storage

$$S(m, n) = \mathcal{O}(m N(m, n)). \quad (11)$$

The key insight is to split the global PIP into:

- a subproblem of dimension $m - 1$ and degree n , and
- a subproblem of dimension m and degree $n - 1$,

and to recurse until only linear ($n = 1$) or univariate ($m = 1$) subproblems remain, both of which admit direct $\mathcal{O}(n^2)$ or $\mathcal{O}(m^2)$ algorithms.

We now sketch how the $\mathcal{O}(N(m, n)^2)$ bound arises from the recursive decomposition. This is not a re-proof of correctness, but a transparent derivation of the runtime for readers unfamiliar with complexity arguments.

Recurrence: Let $T(m, n)$ denote the number of arithmetic operations performed by PIP-SOLVER (Hecht et al., 2017) for parameters (m, n) . The algorithm performs three main types of work:

1. Solve a subproblem on a hyperplane $H \cong \mathbb{R}^{m-1}$ with parameters $(m - 1, n)$, costing $T(m - 1, n)$.
2. Solve a subproblem in full dimension with reduced degree, parameters $(m, n - 1)$, costing $T(m, n - 1)$.
3. Combine the two solutions into the global interpolant Q , which involves a linear number of operations per coefficient.

The decomposition is structured so that the total number of nodes used by the two subproblems equals the total number of nodes of the original problem:

$$N(m - 1, n) + N(m, n - 1) = N(m, n). \quad (12)$$

This identity is easy to verify directly from (9):

$$\binom{m - 1 + n}{n} + \binom{m + n - 1}{n - 1} = \binom{m + n}{n}.$$

The combination step (forming $Q = Q_1 + Q_H Q_2$ in the notation of Hecht et al.) requires multiplying a linear polynomial Q_H by a polynomial with $N(m, n - 1)$ coefficients and then adding this to a polynomial with $N(m - 1, n)$ coefficients. This can be done in a number of arithmetic operations proportional to

$$C_3 N(m - 1, n) N(m, n - 1)$$

for some constant C_3 , because each coefficient of the product depends on a constant number of coefficients of the factors and there are $N(m - 1, n)$ and $N(m, n - 1)$ coefficients to process.

Altogether, we obtain a recurrence of the form

$$T(m, n) \leq T(m - 1, n) + T(m, n - 1) + C_3 N(m - 1, n) N(m, n - 1), \quad (13)$$

for $m, n > 1$, with base cases $T(1, n) = \mathcal{O}(n^2)$ and $T(m, 1) = \mathcal{O}(m^2)$ as discussed in the main text (univariate and linear interpolation).

Big- \mathcal{O} and Θ notation: For clarity: for two non-negative functions A, B of our parameters,

- $A = \mathcal{O}(B)$ means that there exists a constant $C > 0$ and a parameter region where $A \leq CB$,
- $A = \Theta(B)$ means $A = \mathcal{O}(B)$ and $B = \mathcal{O}(A)$. In other words, A and B are bounded above and below by constant multiples of each other.

We will show that $T(m, n)$ grows on the order of $N(m, n)^2$.

Induction hypothesis: Assume there exists a constant $C > 0$ such that for all smaller parameter pairs (m', n') (in the sense $N(m', n') < N(m, n)$) we have

$$T(m', n') \leq C N(m', n')^2. \quad (14)$$

This holds for the base cases by choosing C large enough.

Bounding the recurrence: Using (13) and the induction hypothesis (14) we obtain for $m, n > 1$:

$$\begin{aligned} T(m, n) &\leq C N(m-1, n)^2 + C N(m, n-1)^2 + C_3 N(m-1, n) N(m, n-1) \\ &= C(N(m-1, n)^2 + N(m, n-1)^2) + C_3 N(m-1, n) N(m, n-1). \end{aligned}$$

Using the identity (12), we can rewrite $N(m, n) = N(m-1, n) + N(m, n-1)$. Then

$$\begin{aligned} N(m, n)^2 &= (N(m-1, n) + N(m, n-1))^2 \\ &= N(m-1, n)^2 + N(m, n-1)^2 + 2 N(m-1, n) N(m, n-1). \end{aligned}$$

Therefore,

$$\begin{aligned} T(m, n) &\leq C(N(m-1, n)^2 + N(m, n-1)^2) + C_3 N(m-1, n) N(m, n-1) \\ &= C N(m, n)^2 + (C_3 - 2C) N(m-1, n) N(m, n-1). \end{aligned}$$

If we choose $C \geq \frac{1}{2}C_3$, then $(C_3 - 2C) \leq 0$, so the last term is non-positive. Hence

$$T(m, n) \leq C N(m, n)^2.$$

By induction, this holds for all m, n , which proves (10). Since the algorithm really does perform at least a constant fraction of these operations, we in fact have the sharper statement

$$T(m, n) = \Theta(N(m, n)^2).$$

H.3. Complexity in terms of grid size D and dimension m :

We now connect the above complexity to a grid of data points. Suppose we have a regular m -dimensional grid with n nodes in each direction, so that the total number of grid points is

$$D := n^m. \quad (15)$$

In practice, we often think of D (the number of samples) and m (the dimension) as given, and wish to understand the cost as a function of these two quantities.

Because n must be an integer, given m and D we define the largest admissible integer degree per dimension as

$$n(D, m) := \max\{n \in \mathbb{N} : n^m \leq D\} = \lfloor D^{1/m} \rfloor. \quad (16)$$

By definition, this implies

$$n(D, m)^m \leq D < (n(D, m) + 1)^m. \quad (17)$$

We then define the corresponding polynomial-space dimension

$$N(m, D) := N(m, n(D, m)) = \binom{m + n(D, m)}{n(D, m)}. \quad (18)$$

Proposition H.2 (Complexity as a function of m and D). *Let $m \geq 1$ and $D \geq 1$ be given and define $n(D, m)$ as in (16). Then the PIP-SOLVER algorithm with degree $n(D, m)$ has runtime*

$$T(m, D) := T(m, n(D, m)) = \Theta(N(m, D)^2) = \Theta\left(\binom{m + n(D, m)}{n(D, m)}^2\right). \quad (19)$$

Proof. By Theorem H.1, $T(m, n(D, m)) = \Theta(N(m, n(D, m))^2)$. The definition (18) identifies $N(m, n(D, m)) = N(m, D)$, which yields (19). \square

For intuition, in the main text one can use the slightly looser but cleaner expression

$$T(m, D) \approx \mathcal{O}\left(\binom{m + D^{1/m}}{m}^2\right),$$

keeping in mind that the exact integer-valued bound is given by (19).

H.4. Asymptotics for fixed m and growing D :

In many applications, the dimension m is fixed while the grid is refined so that $D \rightarrow \infty$. We now show that in this regime the cost is essentially quadratic in the number of grid points.

Recall that

$$N(m, n) = \binom{m + n}{n} = \frac{(n+1)(n+2) \cdots (n+m)}{m!}.$$

Factor out n^m :

$$N(m, n) = \frac{n^m}{m!} \prod_{k=1}^m \left(1 + \frac{k}{n}\right). \quad (20)$$

For fixed m and $n \rightarrow \infty$, each factor $1 + \frac{k}{n} \rightarrow 1$. Using the Taylor expansion $\log(1 + x) = x + \mathcal{O}(x^2)$ as $x \rightarrow 0$, we obtain

$$\log \prod_{k=1}^m \left(1 + \frac{k}{n}\right) = \sum_{k=1}^m \log\left(1 + \frac{k}{n}\right) = \mathcal{O}\left(\frac{1}{n}\right),$$

hence

$$\prod_{k=1}^m \left(1 + \frac{k}{n}\right) = 1 + \mathcal{O}\left(\frac{1}{n}\right).$$

Substituting this into (20) gives

$$N(m, n) = \frac{n^m}{m!} \left(1 + \mathcal{O}\left(\frac{1}{n}\right)\right) \quad (n \rightarrow \infty, m \text{ fixed}). \quad (21)$$

Now set $n = n(D, m)$. From (17) we have $n(D, m)^m \sim D$, so

$$n(D, m) = D^{1/m} (1 + o(1)) \quad (D \rightarrow \infty).$$

Plugging this into (21) yields

$$N(m, D) = \frac{D}{m!} (1 + o(1)), \quad D \rightarrow \infty, m \text{ fixed}. \quad (22)$$

Combining (22) with $T(m, D) = \Theta(N(m, D)^2)$ gives:

Corollary H.3 (Fixed m , growing grid). *For fixed dimension m and $D \rightarrow \infty$,*

$$T(m, D) = \Theta\left(\frac{D^2}{(m!)^2}\right) = \Theta(D^2). \quad (23)$$

Thus, for fixed m the runtime is asymptotically quadratic in the number of grid points D .

H.5. Asymptotics for fixed D and growing m :

The complementary regime is to fix the grid budget $D > 1$ and let the dimension m increase. In this case we cannot keep n large: the per-dimension degree must shrink, and eventually we are forced into degree 1.

Lemma H.4 (Degree collapse for fixed budget). *Fix $D > 1$ and define $n(D, m)$ by (16). Then there exists*

$$M(D) := \lfloor \log_2 D \rfloor + 1$$

such that

$$n(D, m) = 1 \quad \text{for all } m \geq M(D).$$

Proof. Suppose $n(D, m) \geq 2$. Then $n(D, m)^m \geq 2^m$. By (17), we also have $n(D, m)^m \leq D$, hence $2^m \leq D$. Thus, if $2^m > D$ we cannot have $n(D, m) \geq 2$; the only possibility is $n(D, m) = 1$.

Choose $M(D) := \lfloor \log_2 D \rfloor + 1$. Then $2^{M(D)} > D$, so for all $m \geq M(D)$ we have $2^m \geq 2^{M(D)} > D$, forcing $n(D, m) = 1$. \square

When $n(D, m) = 1$, the polynomial space is simply the affine functions

$$p(x) = a_0 + \sum_{j=1}^m a_j x_j,$$

with dimension

$$N(m, 1) = \binom{m+1}{1} = m+1. \quad (24)$$

Therefore, by Theorem H.1,

$$T(m, 1) = \Theta(N(m, 1)^2) = \Theta((m+1)^2) = \Theta(m^2).$$

Combining this with Lemma H.4 yields:

Theorem H.5 (Fixed budget, increasing dimension). *Fix a grid budget $D > 1$ and let $n(D, m)$ be defined as in (16). Then the runtime of PIP-SOLVER satisfies*

$$T(m, D) = T(m, n(D, m)) = \Theta(m^2) \quad \text{for all } m \geq M(D), \quad (25)$$

where $M(D) = \lfloor \log_2 D \rfloor + 1$. In words, under a fixed grid budget, the interpolation cost grows only quadratically in the dimension m once m is large enough.

To summarize, in terms of the dimension m and the grid budget D :

- The *exact* runtime of multivariate Newton interpolation using PIP-SOLVER with degree $n(D, m)$ is

$$T(m, D) = \Theta\left(\binom{m+n(D, m)}{n(D, m)}^2\right), \quad n(D, m) = \lfloor D^{1/m} \rfloor.$$

- For fixed m and $D \rightarrow \infty$, the runtime is asymptotically quadratic in the number of grid points:

$$T(m, D) = \Theta(D^2).$$

- For fixed D and $m \rightarrow \infty$, the admissible degree collapses to 1 and the runtime is asymptotically quadratic in the dimension:

$$T(m, D) = \Theta(m^2) \quad (m \geq M(D)).$$